

May 1982

Electron-Proton Interaction Experiment

- Argonne National Laboratory
 Y. Cho, E. Crosbie, M. Foss
Carleton University
 K. Edwards
Chalk River Nuclear Laboratory
 J. McKeown
University of Colorado
 P. Coteus, U. Nauenberg
Columbia University
 M. Atiya, S. Holmes, B. Kwan, W. Lee, F. Sciulli, R. Seto,
 M. Shaevitz, W. Sippach, G. Tzanakos, R.R. Wilson
Fermi National Accelerator Laboratory
 M. Harrison, D. Johnson, P. Limon, F. Mills,
 J. Peoples, A. Ruggiero, A. Russell
Harvard University
 J. Rohlf, R. Wilson
University of Illinois
 M. Lamm, T. O'Halloran, J. Wiss
Johns Hopkins University
 A. Pevsner
University of Maryland
 A. Skuja
McGill University
 S. Conetti, D. Stairs
University of Michigan
 R. Gustafson
Michigan State University
 M. Abolins, D. Owen
NIKHEF-H, Amsterdam
 H. Paar, M.E.J. Wigmans
University of Pennsylvania
 W. Kononenko, W. Selove, G. Theodosiou
Princeton University
 B. Louis, K. McDonald, F. Shoemaker, D. Stickland
Rice University
 J. Roberts
Rockefeller University
 S. White
Saclay
 J. Feltesse, A. Givernaud, A. Leveque,
 A. Milsztajn, P. Verrechia
University of Saskatchewan
 R. Servranckx
University of Toronto
 V. Elias, N. Isgur, J. Martin, P. Padley

Spokesmen: W. Lee, D. Stairs, R. R. Wilson

Table of Contents

	<u>Page</u>
I. <u>Introduction</u>	1
II. <u>The Physics</u>	3
III. <u>The Electron Storage Ring</u>	14
<u>Issues Arising from the P 708 Storage Ring Design</u>	
A. Bypass	15
B. Luminosity/Beam-Beam Interactions	16
C. Beam Stability/Injection	17
D. Chromaticity	17
E. Vacuum	18
F. Polarization	18
<u>Current 5 GeV Storage Ring Design</u>	
A. Lattice	20
B. Beam-Beam Interaction	30
C. Beam Stability	30
D. Chromaticity	34
E. Vacuum	38
F. Injection	39
G. Proton Insertion	40
IV. <u>A Detector for $5 \times 1000 \text{ GeV}^2$ e-p Collisions</u>	42
V. <u>Running Scenario</u>	57
VI. <u>Costs</u>	61
VII. <u>Summary</u>	64
<u>Acknowledgments</u>	65

I. Introduction

This document has been prepared jointly by the Canadian and the U.S. e-p groups. It is a direct outgrowth of the three proposals (P 659, P 703, P 708) submitted by these groups to Fermilab advocating the construction of an e-p collider. Since the submission of P 708 in November 1981, a great deal of effort has gone into developing a better understanding of the physics potential of the $5 \times 1000 \text{ GeV}^2$ e-p collider and the associated detector. We have also worked to modify the electron ring design in order to answer questions raised by machine experts regarding the P 708 5 GeV storage ring design, and have developed a definite running scenario which allows maximal utilization of the expected six to eight weeks a year available for e-p running.

In Chapter II we discuss the physics of e-p; in Chapter III we present a modified electron ring design which addresses most of the criticisms raised by the P 708 design; in Chapter IV we describe the detector appropriate for studying the physics; and in Chapter V we describe a running scenario in which we expect to study $5 \times 1000 \text{ GeV}^2$ electron-proton collisions with a minimum of interference with the Tev I and the Tev II programs. Many of the issues discussed here are specific to the 5 GeV electron energy. Much more general (and lengthy) discussion may be found in the above mentioned proposals. Chapter VI discusses our cost estimates.

We hope for immediate approval of the $5 \times 1000 \text{ GeV}^2$ electron-proton collider at Fermilab: approval now will allow for construction of the electron storage ring and detector by the end of 1985 with physics commencing in 1986. We believe it is essential that there be parallel efforts in the study of lepton-lepton, quark-quark, and lepton-quark interactions at ever increasing energies. The facility described here combines enormous near term potential for new and interesting physics with an almost unlimited opportunity for future extension.

II. The Physics

While it is remarkable that the "standard theory" is in accord with our present knowledge of physics, it must be recognized that the state of our present knowledge is in some ways very rudimentary. To critically test the standard theory will require new instruments like the current generation of high energy colliders. We believe that e-p colliders have a very important role to play in testing the standard theory and, in general, in exploring new domains of energy and momentum transfer.

In the scenario in which we imagine that the next decade of experimentation leads to the confirmation of the standard theory, this e-p collider and its successors could:

1. measure M_W and M_Z via space-like propagator effects,
2. observe parity and charge conjugation asymmetries of order unity,
3. measure the Q^2 dependence of the proton structure functions to test the QCD anomalous dimensions without confusion from power law effects,
4. measure $R(x, Q^2) \equiv \sigma_L / \sigma_T$,
5. measure multiple jet cross sections and see jet broadening,
6. study the fragmentation functions of u and d quarks and their Q^2 dependence,
7. produce new quarks,

8. measure or set limits on the Kobayashi-Maskawa angles for $u \leftrightarrow b$, $d \leftrightarrow t$, the $b \leftrightarrow t$ transitions,
9. observe real photon QCD processes and measure the photon structure functions,
10. study γp interactions,
11. establish the validity of QED in new domains,
12. study quark hadronization, and
13. much else besides.

A similarly impressive (but necessarily much more speculative) list of capabilities of the e-p collider could be produced by imagining various scenarios leading to the collapse of the standard theory. In Tables II-1 and II-2 we try to further delineate the important role which could be played by e-p colliders by listing their capabilities in comparison with other sorts of colliders. Clearly these tables are in accord with the lesson of history: just as in the past, the physics issues addressed by lepton-quark colliders will be complementary to those accessible in (already approved) lepton-lepton and quark-quark colliders. The modest $5 \times 1000 \text{ GeV}^2$ collider we are proposing here can, as shown in what follows, make a good beginning at this task.

In the running scenario described in Chapter V, we anticipate (as we do in what follows) an initial run of 1000 hours with a peak luminosity of $4 \times 10^{31} \text{ cm}^{-2} \text{ sec}^{-1}$ leading to an integrated luminosity of $4 \times 10^4 \text{ nb}^{-1}$. We

Table II-1: e-p Colliders in the Scenario of Consolidation

<u>Measurement</u>	<u>Tests</u>	<u>$\int \mathcal{L} dt$ required</u>	<u>Other Sources</u>
$f_i(x, Q^2)$	QCD elementarity	small	none
$e \rightarrow \nu_e$	GWS	small	none
$e \rightarrow e$	GWS QED	moderate	$e^+ e^-$
γp	QCD photophysics hadron-hadron	small-large	none
$q \rightarrow$ hadrons	QCD confinement models	small	all (probably)
jets	QCD confinement models	moderate	all
new quarks	standard theory	large	all
$q-q'$ mixing	standard theory	very large	all

Table II-2: e-p Colliders in the Scenario of Collapse

<u>Measurement</u>	<u>Tests</u>	<u>$\int \mathcal{L} dt$ required</u>	<u>Other Sources</u>
$e \rightarrow e^*$ (Neutral)	extended families e elementarity	small	none
$f_i(x, Q^2)$	q elementarity	small	none
mult. Z^0, W^\pm	GWS	moderate (w/e^+e^-)	all
$e_R^- \rightarrow \nu_e$	L-R symmetry	small ($m_{\nu_e} \gg 0$)	none
$q \rightarrow q^*$	extended families q elementarity	moderate	all
free quarks	!	?	all
new phenomena	?	?	?

also consider a hypothetical integrated luminosity of 10^6 nb^{-1} which might be attainable over the lifetime of the facility.

The broad range of physics issues which could be addressed by an e-p collider has been mentioned above and extensively discussed in previous proposals. Here we concentrate on a few simple issues that have now been the most thoroughly studied by Monte Carlo techniques: the measurement of the neutral current and charged current cross sections which form the backbone of the experiment.

Figures II-1 show the expected number of deep inelastic events with $Q^2 > Q_0^2$ as a function of Q_0^2 ; Fig. II-1a shows for comparison the expectations for a similar run with the Tevatron muon beam. These events are of course rich in physics. For example, comparison of e^- and e^+ neutral current running would (in the standard picture) reveal large C violations from Z^0 exchange. As a further example, Figs. II-2 show a simulated data set of charged current events from such runs binned in x as a function of Q^2 . This latter measurement is especially interesting since it represents essentially a direct measurement of the underlying quark x -distribution function.

There are many other measurements which be available to this e-p collider and these are also under study via Monte Carlo techniques. For example, the collider will produce a high luminosity tagged photon beam (with laboratory

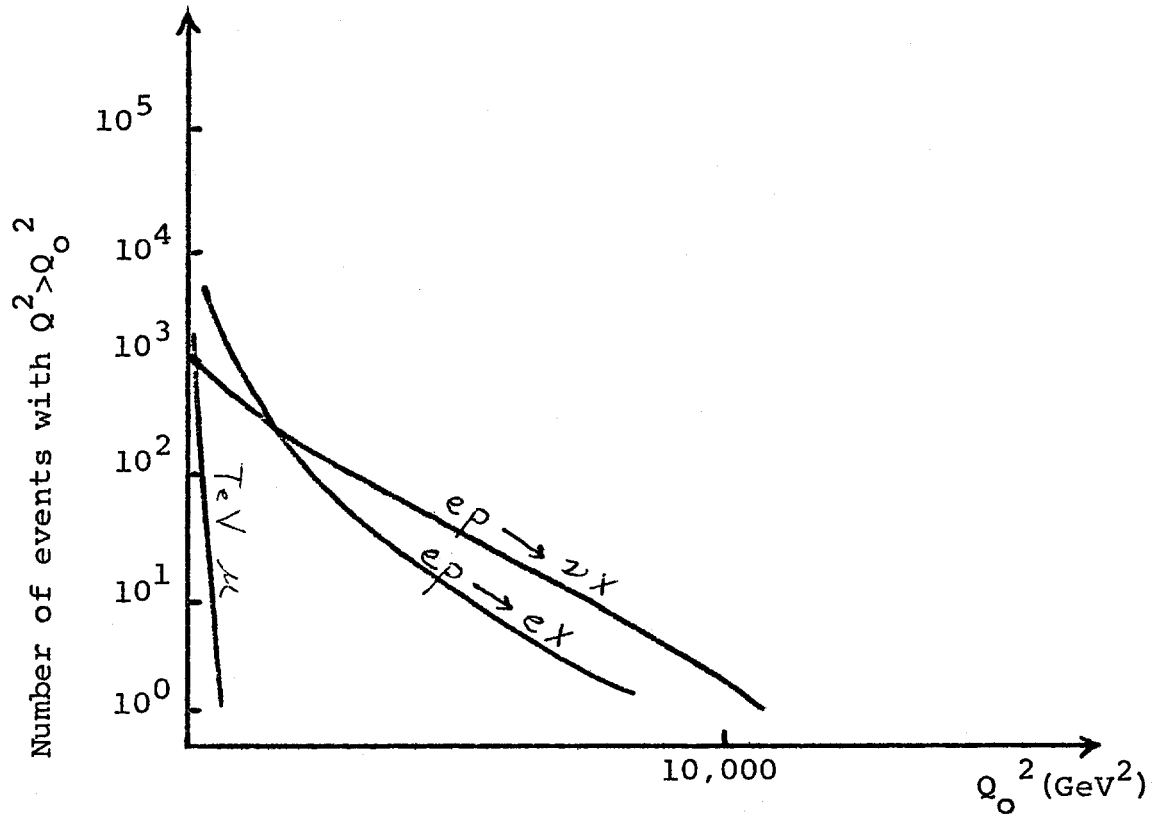


Fig.II-1a: The number of events w/ $Q^2 > Q_0^2$ for a hypothetical initial run w/ $\int \mathcal{L} dt = 4 \times 10^4 \text{ nb}^{-1}$. The expected number of events for a similar length run with the Tevatron muon beam is shown for comparison.

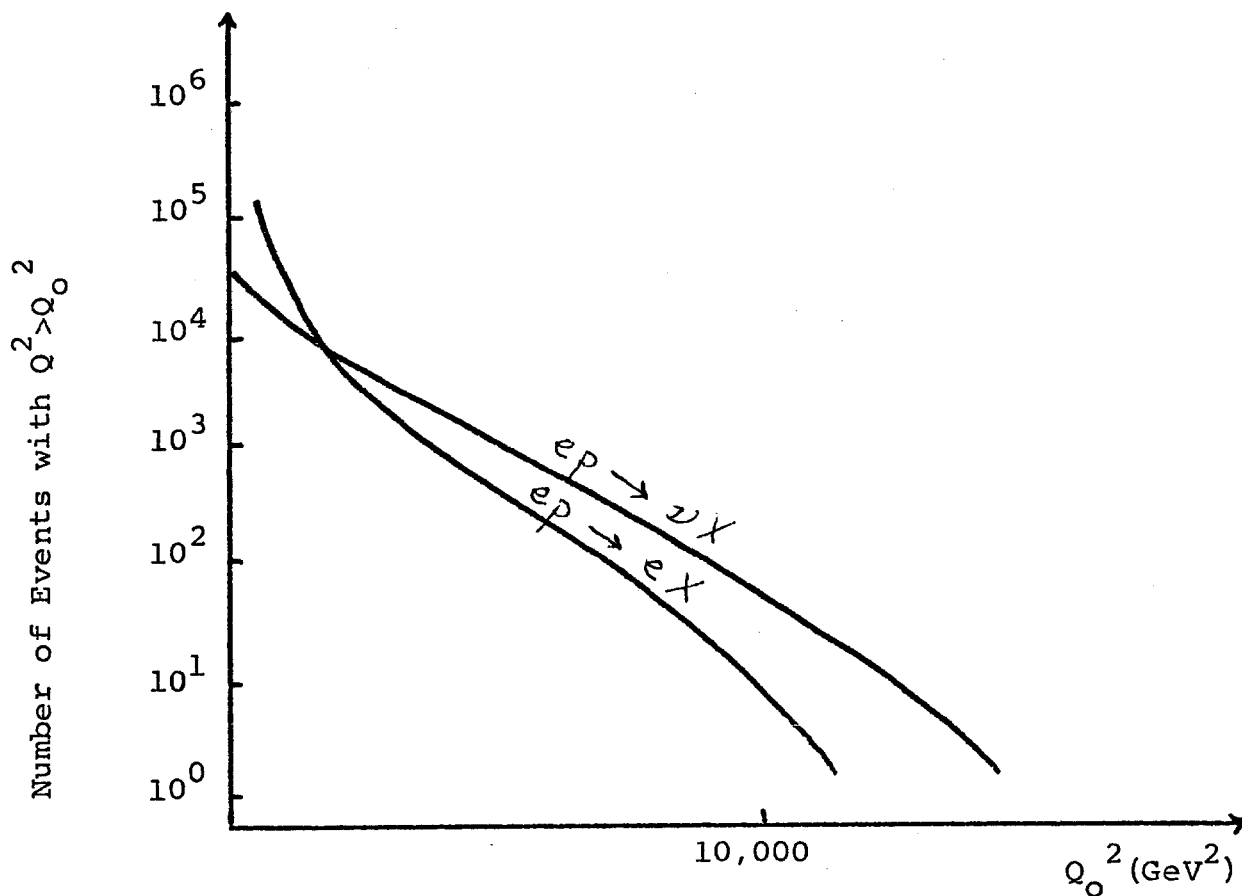


Fig.II-1b: The number of events with $Q^2 > Q_0^2$ for a hypothetical cumulative run with $\int \mathcal{L} dt = 10^{60} \text{ nb}^{-1}$.

Fig. II-2a: The number of events observed in $e^-p \rightarrow \nu_e X$ as a function of X for various Q^2 ranges for a hypothetical initial run of $\int \mathcal{L} dt = 4 \times 10^4 \text{ nb}^{-1}$: $\bar{X} = 400 \leq Q^2 (\text{GeV}^2) \leq 4,000$; $\bar{Q} = 4,000 \leq Q^2 (\text{GeV}^2) \leq 10,000$. Statistical errors are too small to show if error flags are absent.

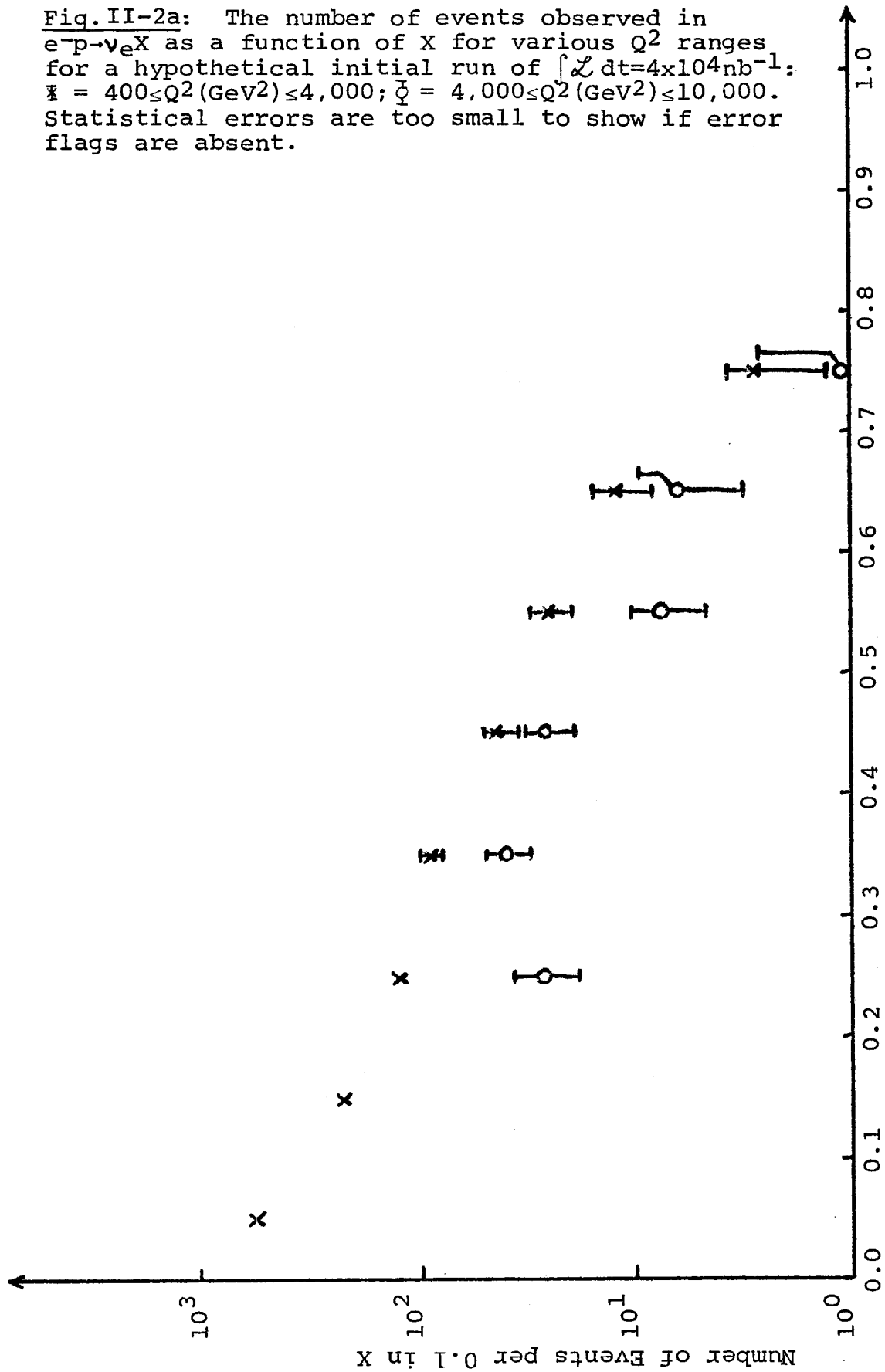
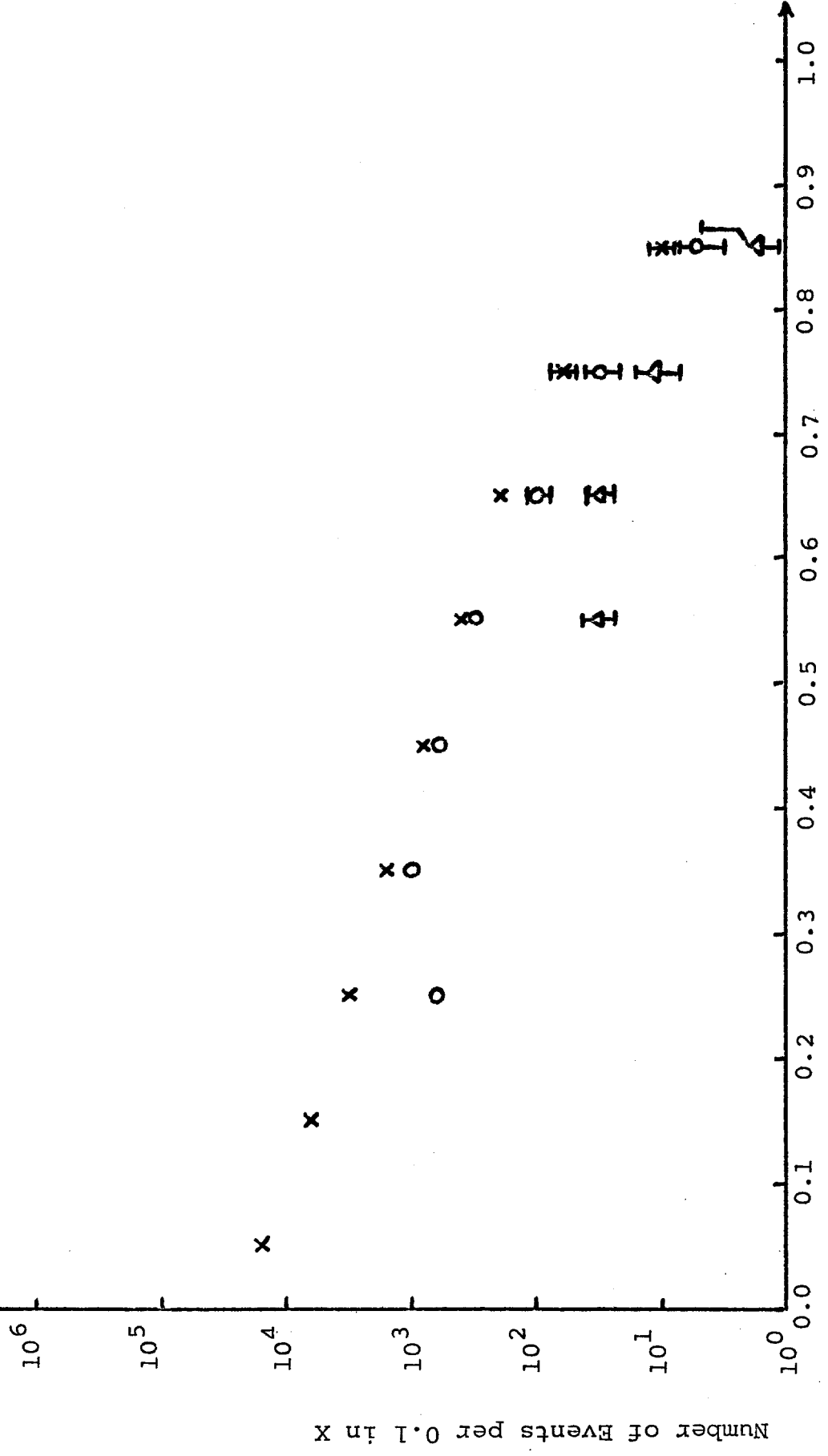


Fig. II-2b: The number of events observed in $e^-p \rightarrow \nu_e X$ as a function of X for various Q^2 ranges for a hypothetical cumulative run of $\int \mathcal{L} dt = 10^6 \text{nb}^{-1}$: $\bar{X} = 400 \leq Q^2 (\text{GeV}^2) \leq 4,000$; $\bar{X} = 4,000 \leq Q^2 (\text{GeV}^2) \leq 10,000$; and $\bar{X} = Q^2 (\text{GeV}^2) > 10,000$. Statistical errors are too small to show if error flags are absent.



equivalent energies of up to 10 TeV) that can be utilized for the study of γp physics. As stressed earlier, the neutral current events will provide invaluable information on quark fragmentation functions since the lepton kinematics allow a prediction of the quark jet direction. We believe that these studies may be indispensable as input to quark jet studies at other colliders. Finally, it is clear that an e-p collider could play a crucial role if the standard theory fails. As an example, Fig. II-3 is a reminder of how subquark structure might be revealed by this experiment if r_q^{-2} is of the order of $10,000 \text{ GeV}^2$.

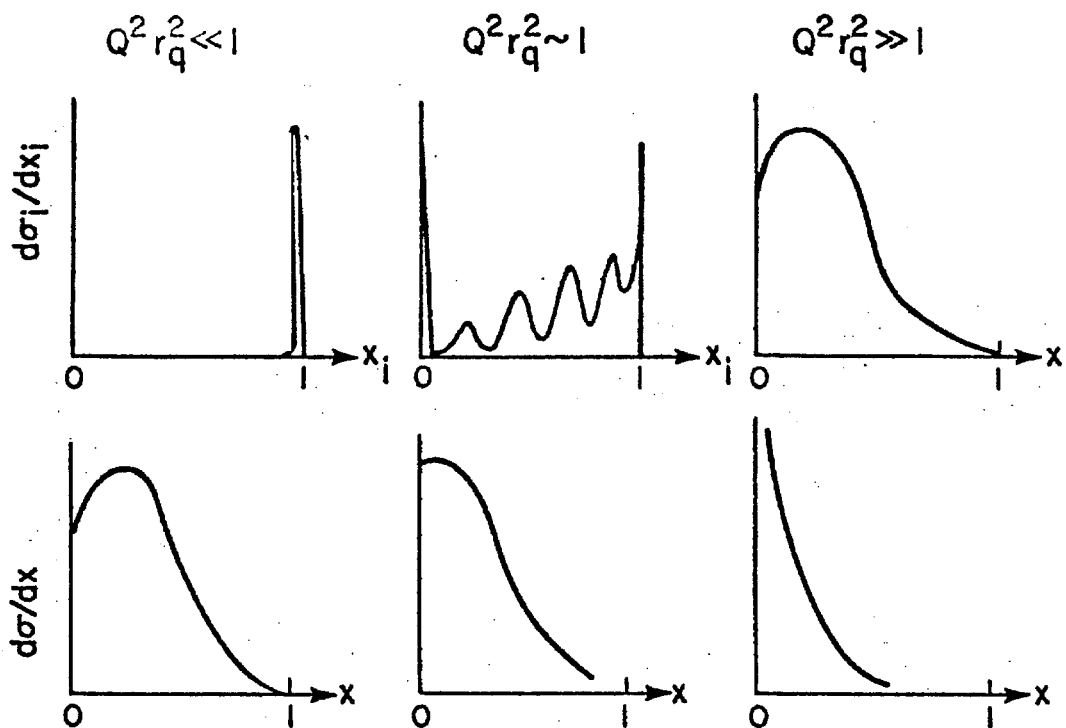


Fig.II-3: An instant replay of history if quarks have substructure with $r_q^{-2} \sim 0$ ($10,000 \text{ GeV}^2$). The top set of diagrams show the evolution of the quark structure function with Q^2 as quark substructure is revealed. This leads to the rapid collapse of the proton structure function shown in the bottom set of diagrams.

III. The Electron Storage Ring

The 5 GeV electron target design presented in P 708 (November 1981) has been subjected to critical review by several authorities on the design and operation of electron storage rings. The views of these people have been communicated both to Fermilab and to our collaboration, and have prompted us to examine more closely certain aspects of the P 708 design and to make modifications where necessary. In addition, we have ourselves reexamined P 708, especially with regard to minimizing the impact of the electron target facility on Tevatron operation while simultaneously providing a reasonable opportunity for studying the physics of e-p interactions. In this section, we first review the questions which have been raised concerning the P 708 design, and then present our solutions in the form of a revised design which appears to have vastly improved operating characteristics without a large increase in the cost.

Issues Arising from the P 708 Storage Ring Design

A. Bypass

The storage ring described in P 708 contained two 40-meter long straight sections, one of which included the interaction point with the other to be used for injection and rf stations. The interaction region straight section contained a 2.2 meter (transverse separation) bypass which was to be used to debug the electron storage ring while the Tevatron was in operation in the Tevatron II running mode. The lattice was designed in such a manner that the bypass could be run in exactly the same configuration as the machine in the e-p interaction mode. This required that the dispersion function and its derivative both be brought to zero at the end of the straight section (see P 708, p. I-23).

Two problems arise with this bypass. First, the 2.2 meter separation between the bypass and the interaction point, i.e. the Tevatron, is insufficient for locating the e-p detector within the bypass for debugging purposes. We now believe that the capability of debugging the detector while Fermilab is running either fixed target or \bar{p} -p is absolutely essential. This requires a bypass which can accommodate at least the central detector and provide electrons and/or positrons, along with room for some amount of shielding. A second problem which arises concerns the natural chromaticity of the lattice. The value of the natural chromaticity of the P 708 ring is ≈ -60 . Approximately -40 of this comes from the interaction region straight section and results from

the requirement that the dispersion and its derivative need to be brought to zero at the end of the straight section. This natural chromaticity is high enough that it would be very hard to correct without reducing the dynamic aperture of the machine at the same time. This problem is described in somewhat more detail below.

Both of these flaws can be remedied by increasing the length of the straight section to about 70 meters, and providing a bypass with a separation of approximately 5 meters.

B. Luminosity/Beam-Beam Interaction

The estimated peak luminosity for electron-proton collisions was given as $4 \times 10^{31} \text{ cm}^{-2} \text{ s}^{-1}$ for the P 708 design. The assumed electron and proton linear tune shifts were 0.03 and 0.002, respectively, and the two beams were assumed to be round. An electron tune shift of 0.03 is consistent with what is observed in the present generation of electron storage rings. However, we know that those rings were designed assuming much higher achievable tune shifts than were actually realized and the result has been luminosities well below the design values. The experience in those rings has also been limited to the use of 'ribbon' beams.

Calculations we have done utilizing computer code written by R. Talman at Cornell now indicate that there is no reason to believe that the design luminosity cannot be attained.

C. Beam Stability/Injection

The design of P 708 called for a circulating electron current of 164 mA and an injection energy of 900 MeV. The fundamental limitations on the electron current obtainable come from the single bunch instabilities. We have estimated the limitations on the electron current arising from three sources: the head-tail instability, bunch lengthening, and Touschek scattering. The estimates are based on extrapolation from SPEAR, PEP, and PETRA and indicate that there is no reason why one cannot expect to be able to store 164 mA at 5 GeV. However, injection of such a current at 900 MeV does not seem possible.

Raising the injection energy to 1.5 - 2.0 GeV seems to be adequate for overcoming the instability problem.

D. Chromaticity

As mentioned above, the natural chromaticity of the ring described in P 708 is about -60. This is extremely high for a ring of 356 m circumference. There are two reasons for the high chromaticity. The first is the presence of the short straight section and associated bypass as described earlier, and the second is that the electron beam required for e-p collisions has a much lower emittance than is generally needed in e^+e^- storage rings. As a result, any 5 GeV electron ring to be used for e-p will have stronger focusing and hence higher chromaticity/circumference than comparable e^+e^- rings.

It is necessary to be able to develop a means of correcting the natural chromaticity of the ring without destroying the dynamical acceptance of the ring in the process. We believe this can be done in a ring which has a circumference of 474 meters ($4/3$ that of the P 708 ring) but with a tune approximately the same as the previously proposed ring.

E. Vacuum

The linear radiated power density in the P 708 ring is 4.6 kW/m. This energy has to be absorbed and then dissipated in the vacuum chamber. In addition this radiation induces desorption in the vacuum chamber walls which provides the bulk of the load on the vacuum system. Experience at CESR and PEP indicates that linear power densities in excess of about 3 kW/m cannot be handled with the simple CESR/PEP style vacuum system.

Again this problem is easily solved by going to a ring of circumference 474 meters.

F. Polarization

In P 708 the idea of producing longitudinally polarized electrons at the interaction point was abandoned because of the inordinately long straight sections needed to accommodate rotators of the form described in the 10 GeV proposal (P 659). However, at 5 GeV it appears that the solenoid based rotator scheme discussed in proposal, P 703, might be

feasible. At 5 GeV the integrated solenoidal field required to rotate the spin through 90° is about 250 kG·m. Although much work would need to be done to find how to fit such a solenoid into the ring without destroying the polarization level itself or the particle orbits, we do not think such an eventuality can be ruled out at the present time.

Current 5 GeV Storage Ring Design

We have looked at two new designs for the 5 GeV electron storage ring. Both have 69 meter straight sections and a bypass with a transverse separation of 4.9 meters. The first ring has the same circumference as P 708 (356 meters) and the second has a circumference of 474 meters. We will discuss only the larger circumference ring since it appears to be superior in all areas (beam stability, rf, vacuum, chromaticity, magnetic field, and operating power) while being virtually identical in cost.

A. Lattice

The current ring has a circumference of 474.2 meters consisting of two 69.0 meter straight sections and two arcs of mean radius 53.5 meters. The machine characteristics are given in Table III-1. The design emittance and values for β_x and β_y at the interaction point are identical to those in P 708, resulting in the same luminosity for the same circulating electron and proton currents. The electron machine now circulates 28 electron bunches assuming the Tevatron has been rebunched by 3. As in P 708, we chose an integer times 7 since this will also allow rebunching by 7 in the Tevatron if that appears advantageous.

The interaction region straight section provides a free space of ± 4.0 meters between the interaction region quadrupoles for insertion of the detector, as in P 708. The

Table III-1: Electron Ring Parameters

<u>Ring</u>	
Energy	5.0 GeV
Number of Bunches	28
Bunch Separation	16.936 m (56.6 ns)
Electrons/Bunch	5.8×10^{10} (164 mA)
Circumference	474.2 m
Emittance (fully coupled) ϵ_x/π	0.065×10^{-6} m
σ_E/E	8.3×10^{-4}
Tune ν_x/ν_y	17/14
Momentum Compaction α	0.00546
Damping Time τ_x	7.3 ms
Polarization Time	27 min
<u>Interaction Region</u>	
β_x/β_y at I.P.	0.25/0.25 m
β_x/β_y max	75/300 m
σ_x/σ_y at I.P.	0.13/0.13 m
<u>rf</u>	
Energy Loss/Turn	2.18 MeV
Voltage	3.8 MV
Frequency	496 MHz (h=784)
ν_s	0.021
σ_z	1.7 cm
Power to Beam	357 kW
Quantum Lifetime	100 hours

layout of the magnets in the interaction area is shown in Figs. III-1 and III-2. Figure III-1 shows the layout assuming that the bypass lies in the horizontal plane. H1 and H2 are horizontal bending magnets which separate the electron and proton beams. Remember that H2 is a septum magnet which also serves to restore the proton beam. As in P 708, we assume that the first Tevatron quadrupole is located 13.5 meters from the interaction point (although this design accommodates Tevatron quadrupoles as close as 12.0 meters from the interaction point).

Because we have brought both the dispersion and its derivative to zero at both the interaction point and the end points, the same lattice can be used to produce a vertical bypass simply by replacing the horizontal dipoles with vertical dipoles and reversing the polarity of all the quadrupoles. The position of the electron, Tevatron, and main ring magnets for such a vertical bypass are shown in Fig. III-2. Note that the electron beam pipe crosses through the main ring beam pipe between the electron quadrupoles Q4 and Q5. At this time the vertical bypass scheme is preferred by us for two reasons. First, since it moves the bypass out of the plane of the Tevatron, it should make shielding of the bypass region much less difficult and so improve access to this region. Second, since the

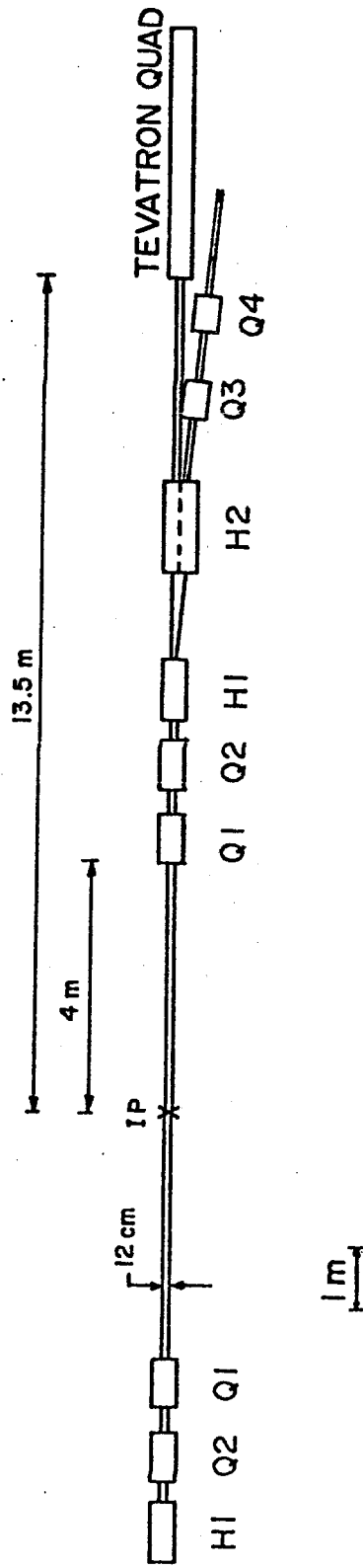


Fig. III-1: The arrangement of electron and proton machine elements near the interaction point (IP) for a horizontal bypass.

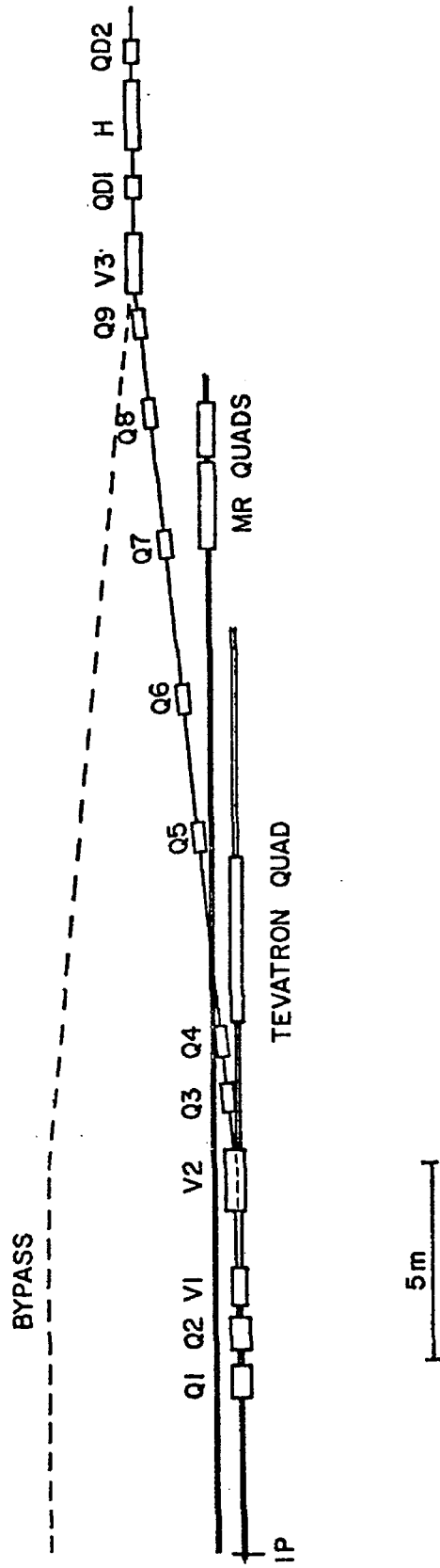


Fig. III-2: The arrangement of electron and proton machine elements near the interaction point (IP) for a vertical bypass.

bypass and tunnel both lie closer to ground level, we expect the associated conventional construction to be less expensive. The electron ring is found to exit the existing tunnel at a position about ± 44 meters from the interaction point. It appears that approximately six of the cast tunnel sections on either side of D0 will need to be modified.

The lattice functions through the interaction region straight section are shown in Fig. III-3. Also shown on the figure are the $\pm 10 \sigma$ beam envelopes in both the horizontal and vertical directions.

The dispersion suppressor and standard FODO cell are shown in Figs. III-4 and III-5. The bending magnets are placed off-center within the cells leaving 80.0 cm and 45.6 cm of free space on either side for placement of sextupoles, beam monitors/controllers, vacuum gauges/pumps, etc. The beam profiles are given on the bottom of the figures. The magnetic field in the dipoles is 6.0 kG ($L = 1.9$ m) and the quadrupole gradient is 135 kG/m ($L = 0.5$ m).

The off-side straight section is shown in Fig. III-6. The straight section is designed with four 6.5 m and one 5.0 m free spaces. These free spaces can be used for injection and installation of the rf system. In particular, the central 5.0 m free space has a nearly constant value of $\beta_x = \beta_y = 10$ m. This low value of β makes it particularly suitable for installation of rf (see discussion on beam stability).

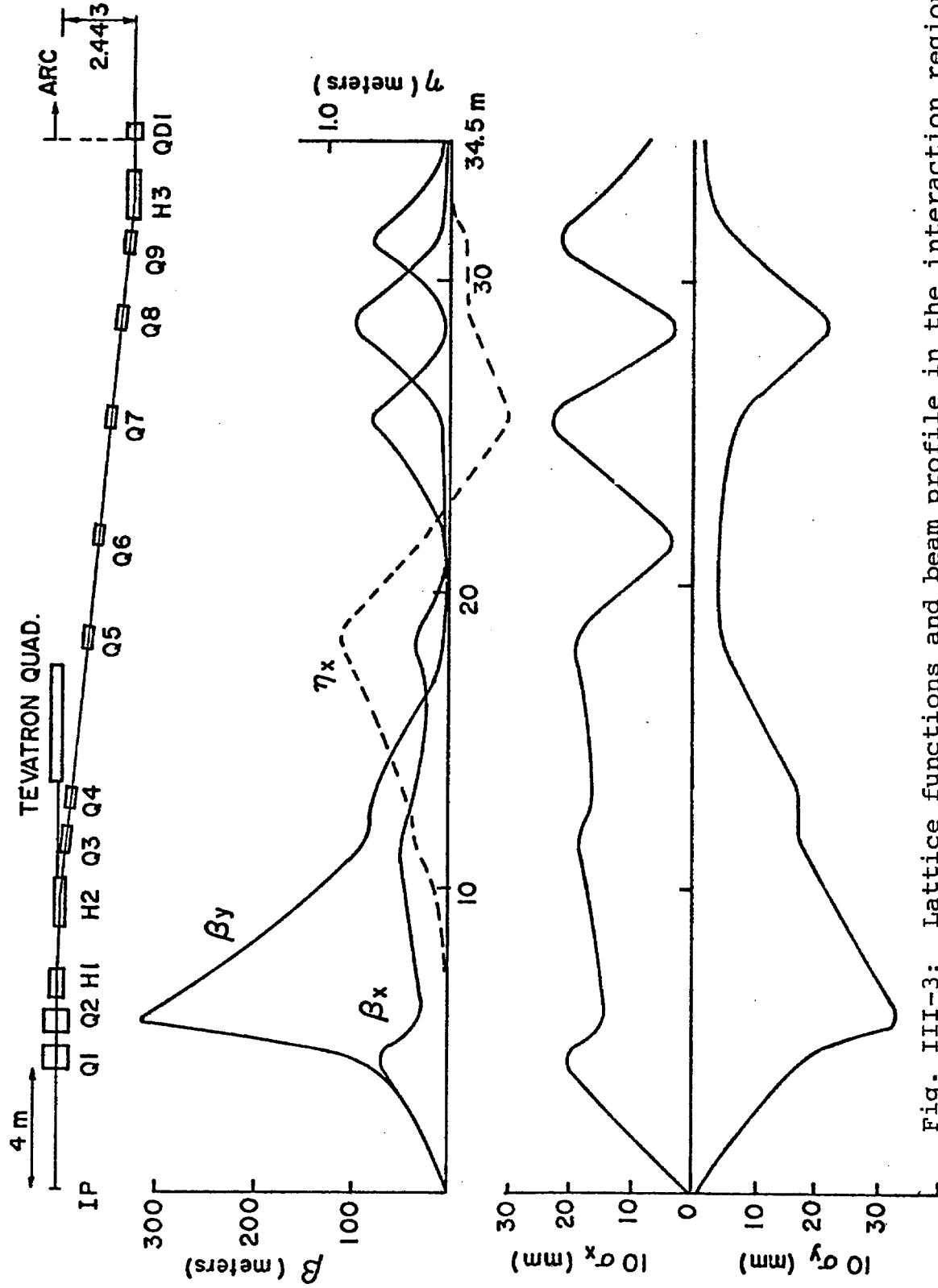


Fig. III-3: Lattice functions and beam profile in the interaction region straight section for the horizontal bypass. For the vertical bypass, x and y are interchanged.

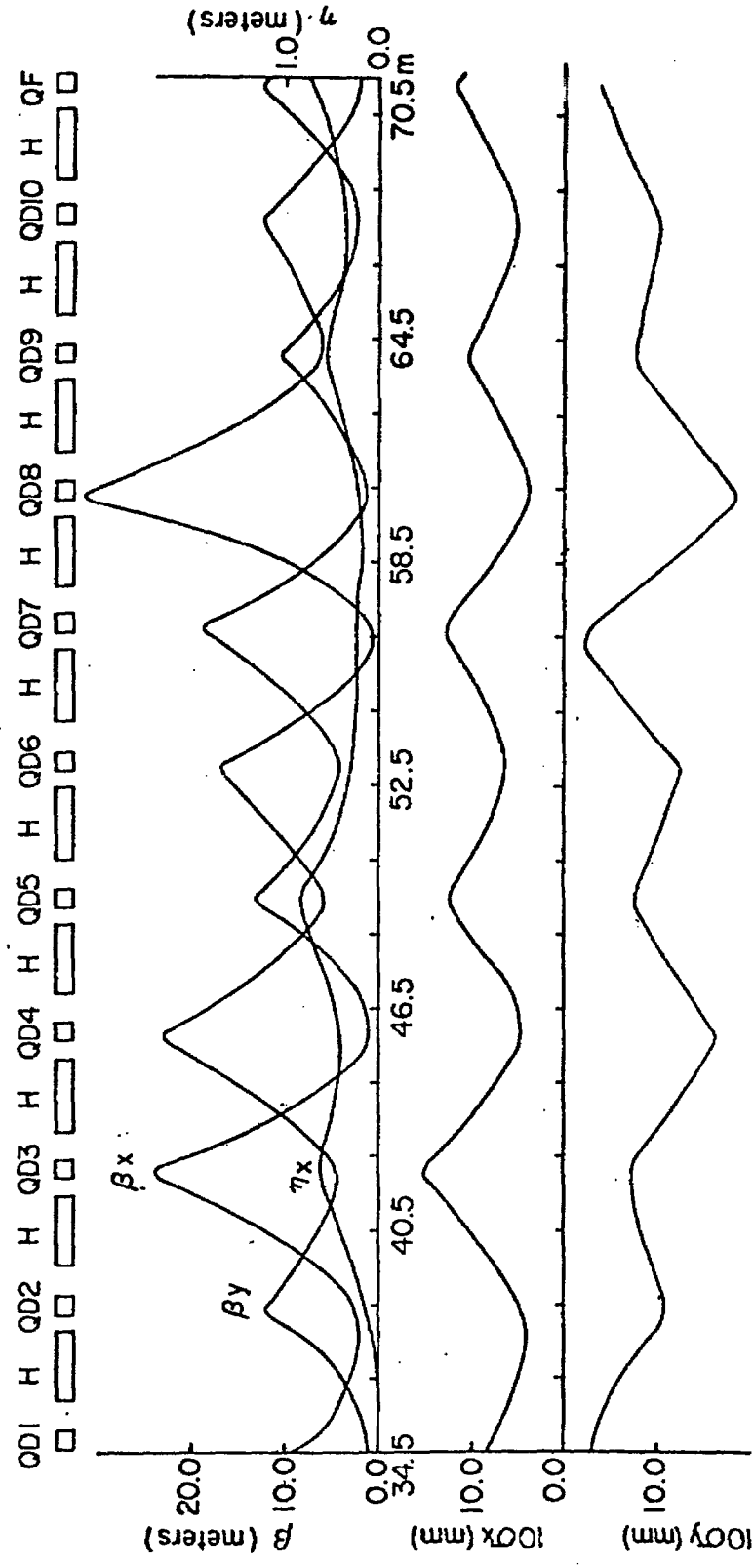


Fig. III-4: Lattice functions and beam profile through the dispersion suppressor.

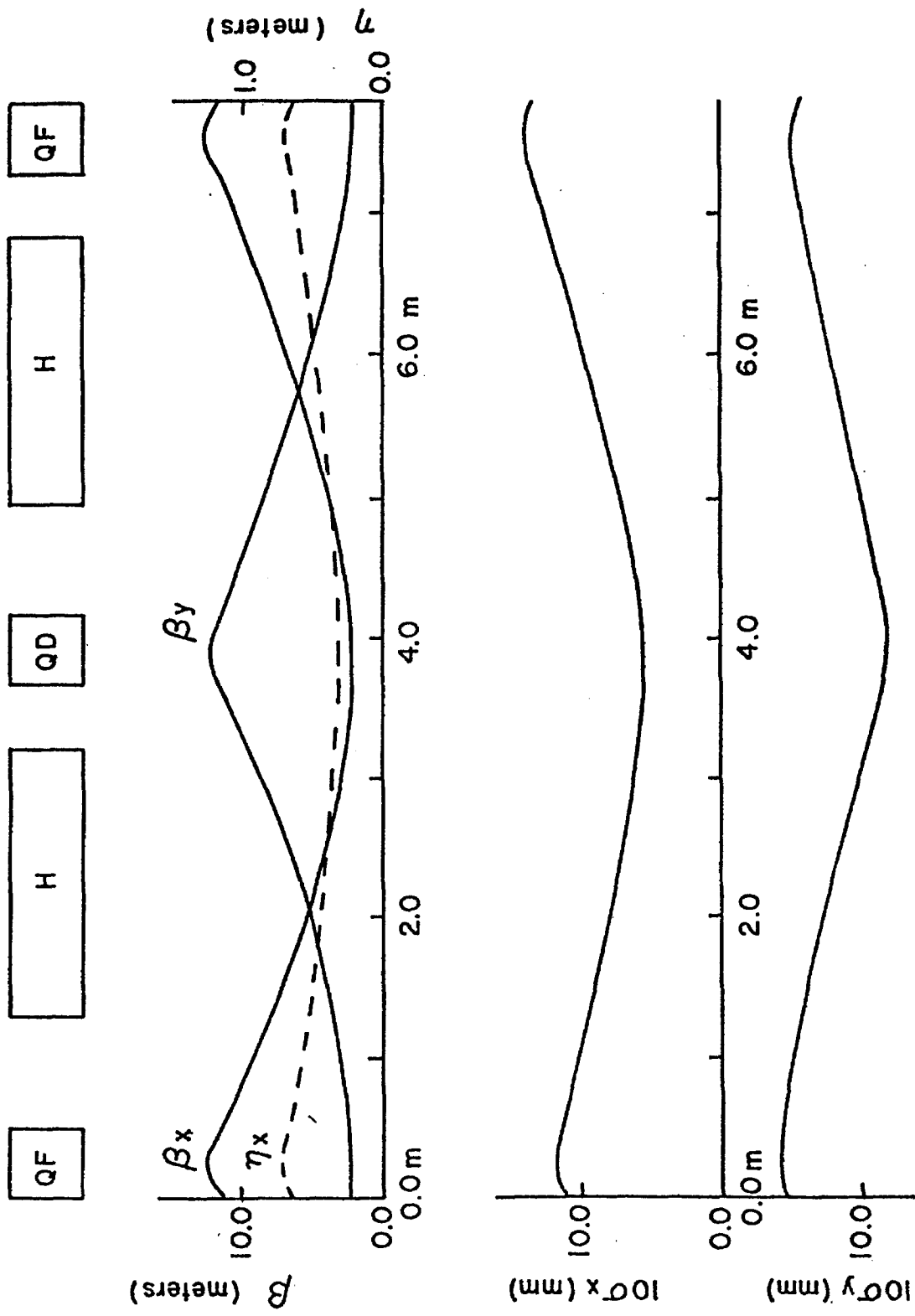


Fig. III-5: The standard FODO cell.

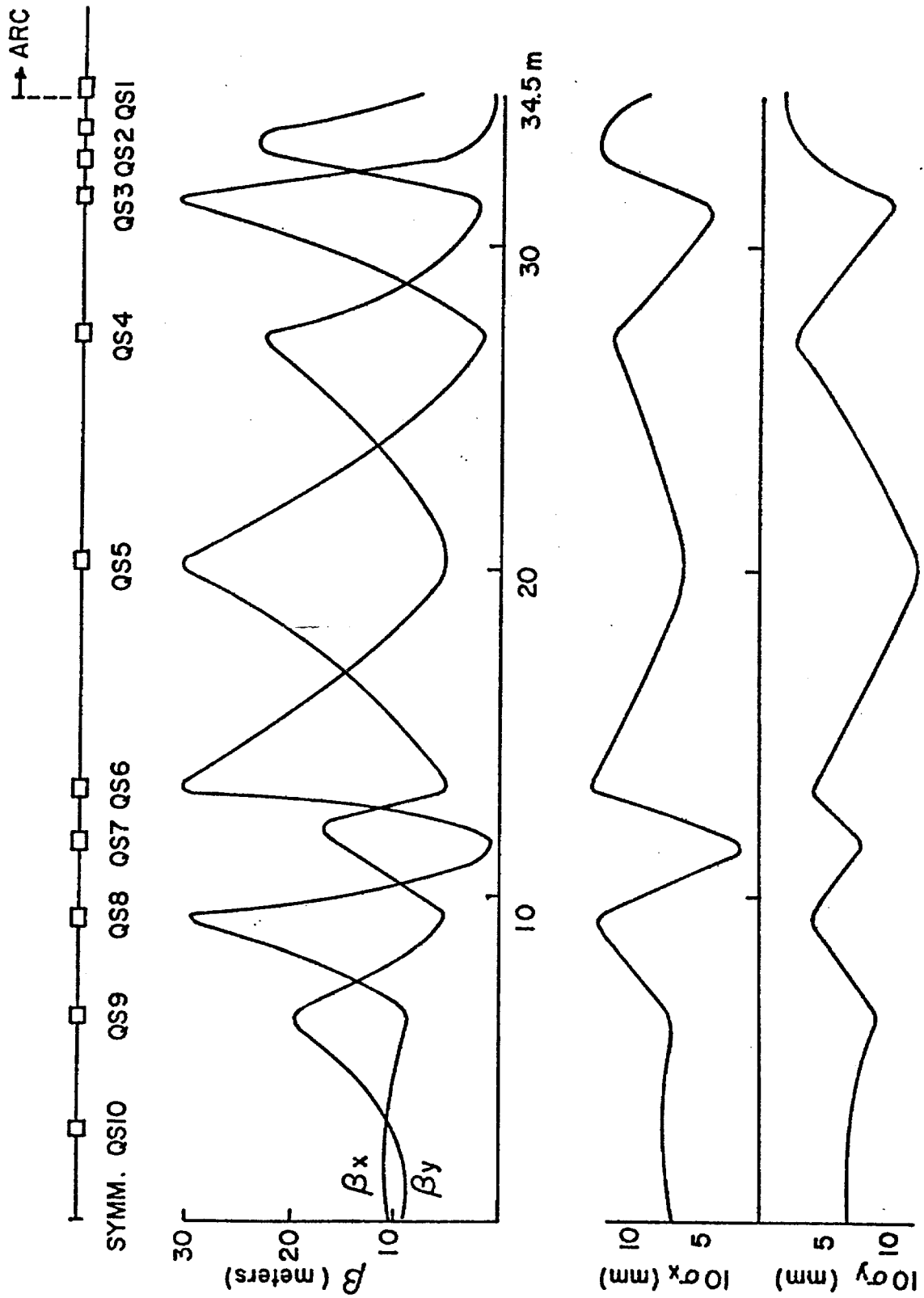


Fig. III-6: Lattice functions and beam profile through the off-side straight section. SYMM is the symmetry point.

B. Beam-Beam Interaction

R. Talman at Cornell has had great success in understanding the observed limitations on circulating electron currents which arise because of the electromagnetic interactions of each beam with the other. He has been able to offer quantitative explanations on the basis of a tracking program which he has developed and which has been recently modified to enable predictions in the case of round beams. We have used this program to investigate the behavior of our 5 GeV electron beam in the presence of the 1 TeV proton beam.

Briefly, the program predicts absolutely no beam blowup (and associated loss in luminosity) under the conditions assumed here, including full x-y coupling. We are now looking to see what the predicted proton intensity threshold and associated potential gain in luminosity are. Since the luminosity of $4 \times 10^{31} \text{ cm}^{-2} \text{ s}^{-1}$ was generated with 2.9×10^{13} circulating protons, there is some possibility for increased luminosity if the protons were to be available.

C. Beam Stability

The beam stability characteristics both at 5 GeV and at 1.5 GeV (injection) are given in Table III-2. We have assumed an rf system based on the CESR design and operating at 496 MHz. The voltage at 5 GeV is chosen to give a quantum lifetime of 100 hours. The voltage at injection is chosen to give the same synchrotron tune as at the full energy. We assume that the rf voltage will have to be programmed to keep v_s constant during ramping.

Table III-2: Beam Stability (rf = 496 MHz)

	<u>5 GeV</u>	<u>1.5 GeV</u>	
U_o	2.18	0.018	MeV
V_{rf}	3.8	0.9	MV
v_s	0.021	0.021	
ϵ/E	5.5×10^{-3}	9.5×10^{-3}	
σ_z	1.66	0.50	cm
N_{cav}	8	8	
β_{rf}	10	10	m
$\tau_{Touschek}$	160 hours	3.0 *	min
$\sigma_{z th}$	0.4	1.0	cm
I_{th}/Bunch	301	25.7	mA
τ_Q	100	∞	hours
R_{SH}	66	66	M Ω
P_{wall}	217	1.2	kW
P_{beam}	358	3.0	kW

* Assumes $\epsilon/E = 0.5\%$, no bunch lengthening.

Gain

x 22 if ϵ/π increases by 10

x 2 if $\sigma_z = 1.0$ cm

x 4 if $\epsilon/E = 0.95\%$.

The Touschek lifetime is given by the formula:

$$\tau = 8\pi\sigma_x\sigma_y\sigma_z\gamma^2/Nr_e^2c(E/\Delta E)^3 D(\epsilon),$$

where

$$\epsilon = \beta^2/2\gamma^2(E/\Delta E)^2\sigma_x\sigma_y, \quad N \text{ is the number of electrons/bunch,}$$

and

$$D(\epsilon) = \sqrt{\epsilon} \left\{ -\frac{3}{2} e^{-\epsilon} + \frac{\epsilon}{2} \int_{\epsilon}^{\infty} \frac{\log u}{ue} du + \frac{1}{2}(3\epsilon - \epsilon \log \epsilon + 2) + \int_{\epsilon}^{\infty} \frac{e^{-u}}{u} du \right\} .$$

The Touschek lifetime at 5 GeV is about 160 hours. However, at the injection energy it is only three minutes. Since we expect positron filling times in the range 10-20 minutes, this is insufficient. Fortunately there are several means by which this time can be increased. First of all, we would anticipate blowing up the transverse dimensions of the beam at injection through the use of wiggler magnets. A factor of 10 increase in the beam emittance at injection results in a factor of 22 increase in the Touschek lifetime. The interaction region straight section is designed with a value of the Courant-Snyder invariant between H2 and H3 (or V2 and V3) which is eight times its average value throughout the whole ring. This means that a factor of ten increase in emittance can be gained by the use of a 15 kG, 40 cm long wiggler in this region. Additionally, it is noted that in the calculation given in Table 2, it is assumed that the bunch length is given by the natural bunch length and the energy acceptance is 0.5% (transverse aperture limited). Indications are that the beam will be subject to bunch lengthening at injection (see below). If this is true, the Touschek lifetime at injection will

increase by another factor of two. Finally, if the limitation on the energy acceptance at injection is the rf system rather than the transverse aperture, another factor of four is obtained. Thus, we are confident that Touschek lifetimes well in excess of an hour can be expected.

Bunch lengthening thresholds are calculated by scaling from SPEAR where the effect has been extensively studied.

The scaling law we use is:

$$\sigma_{th} \text{ (cm)} = 2.6 \times 10^{-6} \left(\frac{i_b \text{ (mA)} \alpha R^3 \text{ (m)}^{.76}}{v_s^2 E \text{ (GeV)}} \right) .$$

This assumes a factor of ten improvement in the vacuum chamber impedance relative to SPEAR. The bunch lengthening thresholds are estimated to be 0.4 cm at 5 GeV and 1.0 cm at 1.5 GeV. Since the natural bunch length is 1.7 cm at 5 GeV and 0.5 cm at 1.5 GeV, we expect bunch lengthening by a factor of two at injection but none at the full energy.

The turbulent threshold for the head-tail instability is estimated by scaling from PETRA and PEP. We use the expression:

$$i_{b_{th}} \text{ (mA)} = 5.2 \times 10^7 \frac{f_s \text{ (kHz)} E \text{ (GeV)} \sigma_z \text{ (cm)}}{n_c f_{rf}^2 \text{ (MHz)} \beta_{rf} \text{ (m)}} .$$

Note that the threshold is proportional to the bunch length, and inversely proportional to the number of rf cavities (n_c) and the value of β through the rf cavities. We have attempted to minimize this effect by keeping β small in the rf region

and by running the rf cavities at a higher gradient (1.6 MeV/m) than is done at CESR in order to reduce the number of cavities. As seen from the Table, the threshold current/bunch is two orders of magnitude greater than required at 5 GeV and about 4.5 times greater than the required current at 1.5 GeV. As in the case of the Touschek lifetime, these thresholds are calculated assuming no bunch lengthening. In the presence of bunch lengthening, we would gain a factor of two at 1.5 GeV.

The only experience with multi-bunch instabilities comes from DORIS and SPEAR. Such instabilities can be dealt with using a large variety of methods including feedback systems, rf quadrupoles, octupoles, and cavity couplers to damp unwanted modes. At DORIS and SPEAR circulating multi-bunch currents in the range of 150-250 mA have been obtained at energies of 1.5-2.5 GeV. We see no reason to believe that such multi-bunch instabilities will provide a fundamental limitation in our 5 GeV ring.

D. Chromaticity

The natural chromaticity in the present ring is -45 horizontally and -42 vertically. This is about 30% lower than in the P 708 design and is attributable to the increased length of the straight section. This is also about a factor of two higher than SPEAR and CESR, but a factor of two lower than PEP. We have investigated the behavior of our ring under various correction procedures using the computer code

PATRICIA (supplied to us by H. Wiedemann at SLAC). PATRICIA is a program which calculates the variation of the betatron tunes and betatron functions with energy and amplitude using a direct matrix method, and the completely coupled synchro-betatron motion of the stored electrons through a tracking procedure. The program also provides a guide as to the positioning and strength of the sextupoles required.

It appears to be very hard to find a solution which corrects the chromaticity of the P 708 ring without losing the stored electrons in the process. The larger circumference ring described here seems to be much better behaved in this respect. In Fig. III-7, we show the variation of the beta functions at the interaction point and the tunes with energy for a particular arrangement of sextupoles (included in five families). Remember that the rms energy spread in the beam is $\pm 0.08\%$ so that ± 10 standard deviations occur at $\pm 0.8\%$ on the plot. The variation in the horizontal tune over the entire range is less than 0.013 while the horizontal beta function varies between 0.23 and 0.33. The variation in the vertical plane is somewhat larger since we have only worked on the horizontal plane so far. We have also looked at the coupled motion using the tracking feature of PATRICIA and found it to be stable out to the largest amplitudes tested (eight standard deviations in x and y, and six standard deviations in ΔE ; see Fig. III-8).

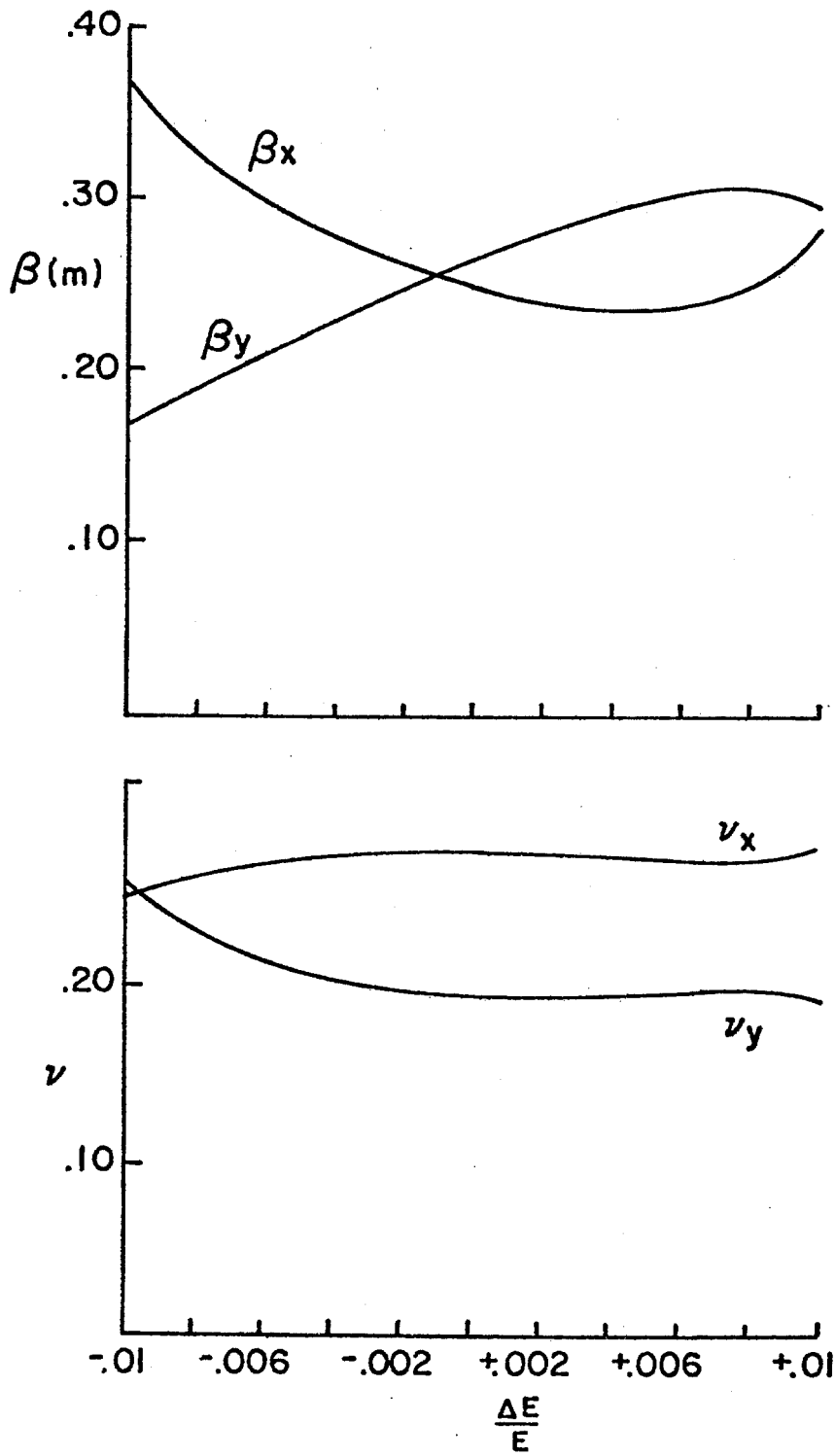


Fig. III-7: Variation of the beta functions at the interaction point and tune with energy for the machine corrected with five families of sextupoles.

The arrangement presented here involves fairly weak sextupoles. The maximum strength required anywhere in the ring is $-4.7/\text{m}^2$ ($3130 \text{ kg}/\text{m}^2$ for a length of 25 cm). We do not believe the arrangement is necessarily optimized at this time. The whole question of chromaticity correction and dynamic aperture is still not well understood by accelerator theorists. Many people advocate several families of sextupoles and attempting to flatten the dependence of β and ν on energy, while others claim that two families with appropriately chosen 'blanks' around the ring is preferable. We believe we have demonstrated a particular solution for our ring and would plan to retain the ability to power all sextupoles independently of each other even if we eventually find a solution involving only two families.

E. Vacuum

The linear power density in the ring is now 1.9 kW/m. This is below the design value of the CESR and PEP rings, although it is higher than the actual operating conditions have allowed at those rings because of the unanticipated current limitations encountered. The actual gas load on the vacuum system due to synchrotron radiation induced desorption from the vacuum chamber walls is calculated to be 6.5×10^{-7} T·L/s/m. This is almost the same as in P 708 and means the desired vacuum of 10^{-8} T is obtained with an installed pumping capacity of 65 L/sec/m.

No specific vacuum chamber design has been completed at this point; but is it worth pointing out that we expect the diameter to be fairly small because of the small beam emittance. We expect a diameter of about 6.0 cm in the arcs of the machine and 12.0 cm in the interaction region.

F. Injection

As stated earlier, we have decided that the injection energy into the 5 GeV ring needs to be raised to about 1.5 GeV (or above). In addition, we would also be more comfortable if we could inject into the booster at ≈ 100 MeV rather than at 40 MeV as proposed initially. We have been investigating the possibility of obtaining some fraction of the Mark III linac from HEPL (Stanford University) and/or the remnants of the Cornell 2 GeV synchrotron which is currently residing at Argonne National Lab.

The Mark III linac at HEPL was originally built as a prototype for SLAC. As such the accelerating cavities are identical to those at SLAC. The linac has been out of commission for several years, but is being revived now for use in a free electron laser project. This project requires only half of the thirty 10 ft sections of the linac, thus freeing approximately fifteen sections. We are currently negotiating to obtain five of these sections for use as an injector into the booster. When driven off a modern SLAC klystron, each 10 ft section is capable of supplying 40 MeV

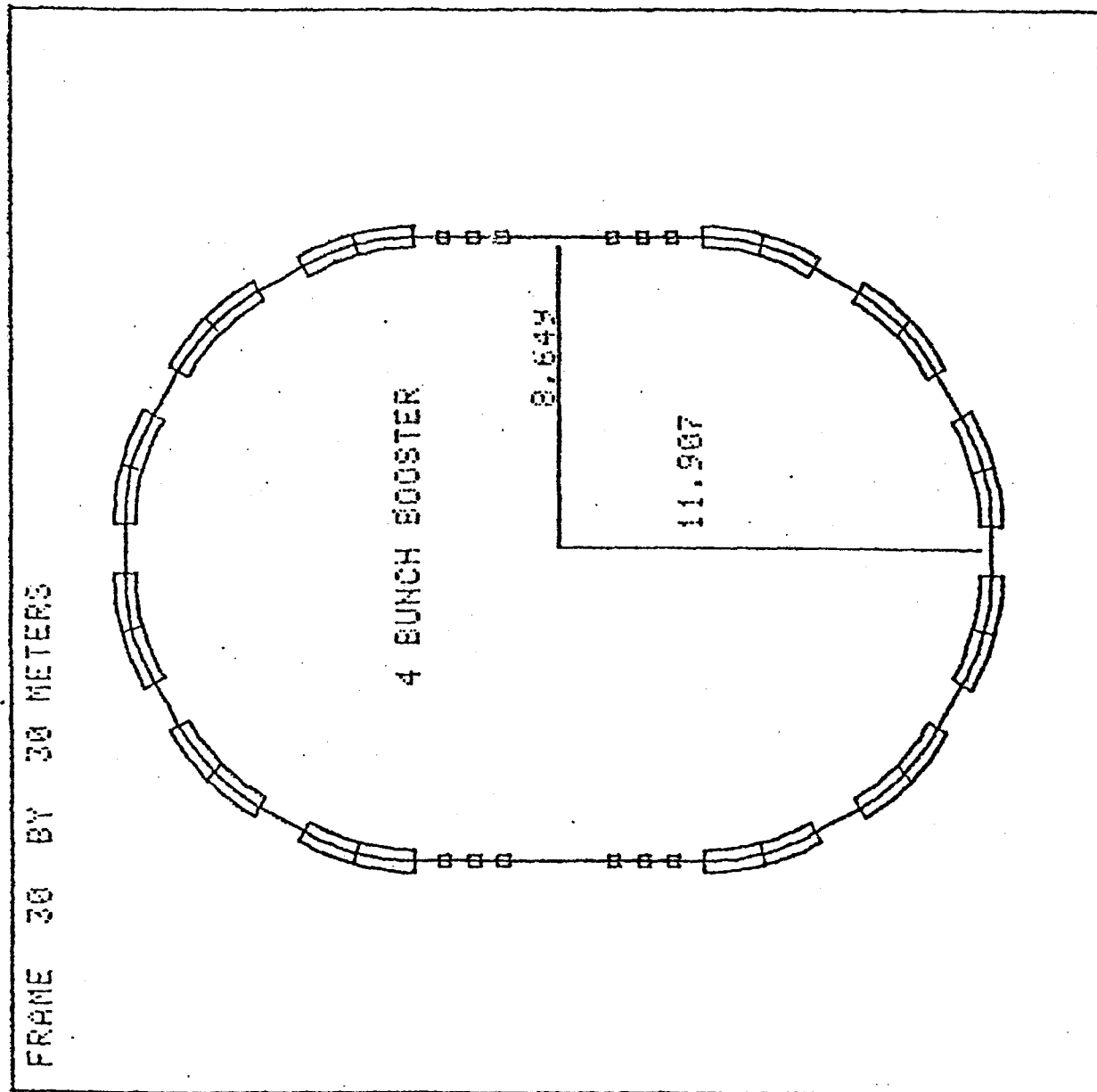
of acceleration. The total available energy of 200 MeV will be very adequate for both electron and positron injection.

The Cornell 2 GeV synchrotron is currently being used as a choke on the Argonne neutron source. We have looked at the practicality of using it as a booster for our 5 GeV storage ring. Figure III-9 shows a possible lattice configuration using the existing gradient magnets with twelve quadrupoles provided in two straight sections to zero the dispersion. The ring shown has a circumference of 68 m (four bunches) and would work fine for electron injection. Whether the aperture is large enough to provide positron filling in a reasonable time is still not clear.

G. Proton Insertion

We reserve the description of the proton insertion for Section V where we discuss possible running scenarios for the e-p experiment and its compatibility with Tev I and Tev II.

Fig. III-9: Geometry of a four bunch booster utilizing the Cornell 2 GeV synchrotron magnets.



IV. A Detector for 5 x 1000 GeV² e-p Collisions

The detector for the 5 x 1000 GeV e-p collider is shown in Fig. IV-1. The design, which is still evolving, is based on the work on the 10 x 1000 collider detectors presented in P 659 and P 703. Our goal is a simple detector for measuring the charged and neutral current differential cross sections. This simple detector can also measure most of the exciting new physics we have considered.

The kinematics of 5 x 1000 e-p collisions can be understood from Figs. IV-2 and IV-3. Here the reactions are approximated by the scattering of a zero mass electron from a zero mass quark carrying the fraction $x E_p$ of the proton momentum. The ellipses in Fig. IV-2 are lines of constant x . These are intersected by lines of constant Q^2 for the final lepton in the upper half and the final current jet in the lower half. The lab angle, P_{\perp} and P_{\parallel} for the lepton and current jet at some x , Q^2 can easily be determined by drawing a line from the origin to the x , Q^2 intersection. An example for $x = 0.3$, $Q^2 = 2500 \text{ GeV}^2$ is shown with lines with arrows, one for the lepton, the other for the current jet. For most of the x , Q^2 region of interest, it can be seen that both the lepton and current jet emerge close to the original proton direction, as expected for such an asymmetric collision.

Figure IV-3 depicts in another way the kinematic range accessible to 5 x 1000 collisions. Lines of

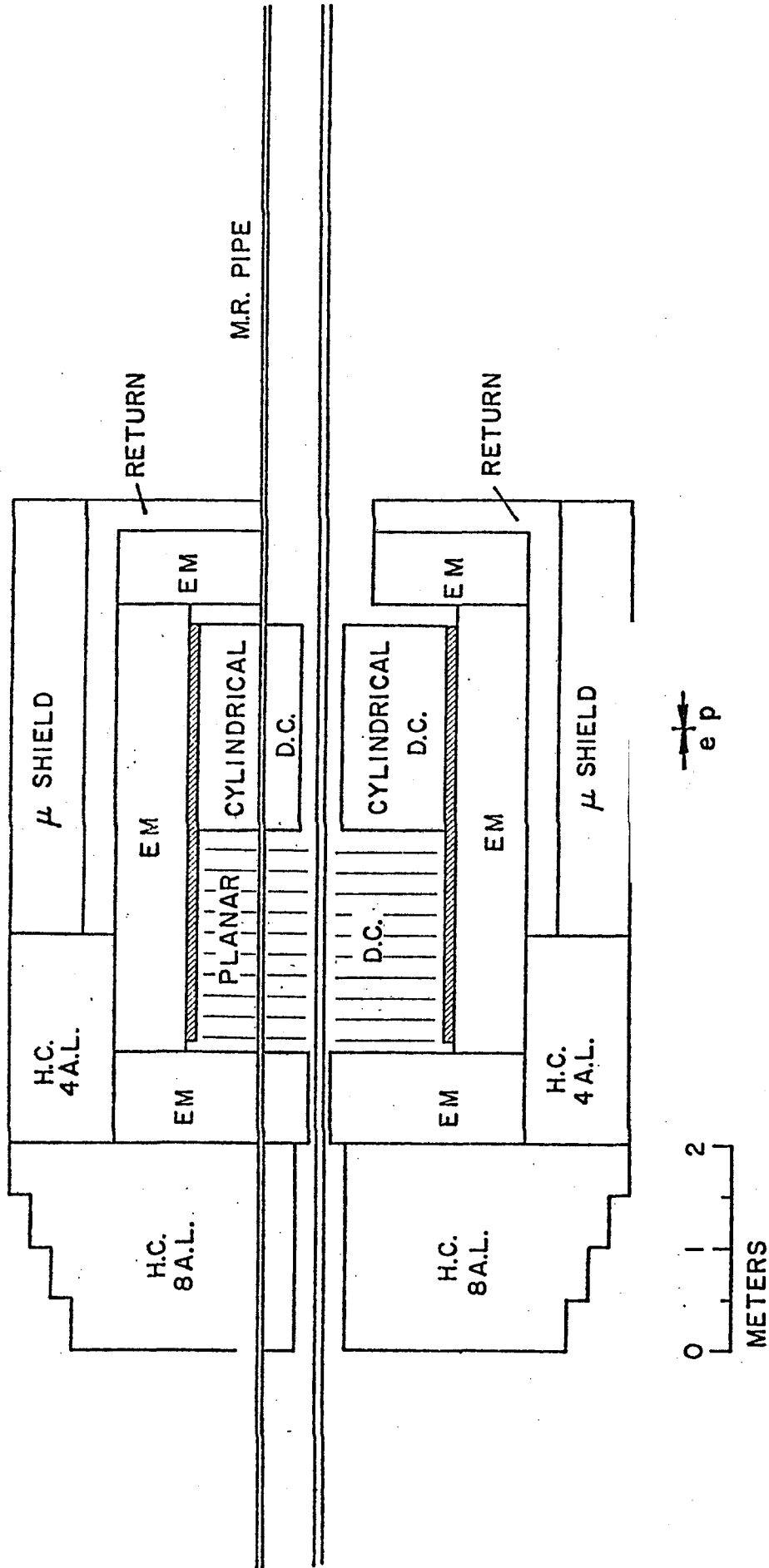
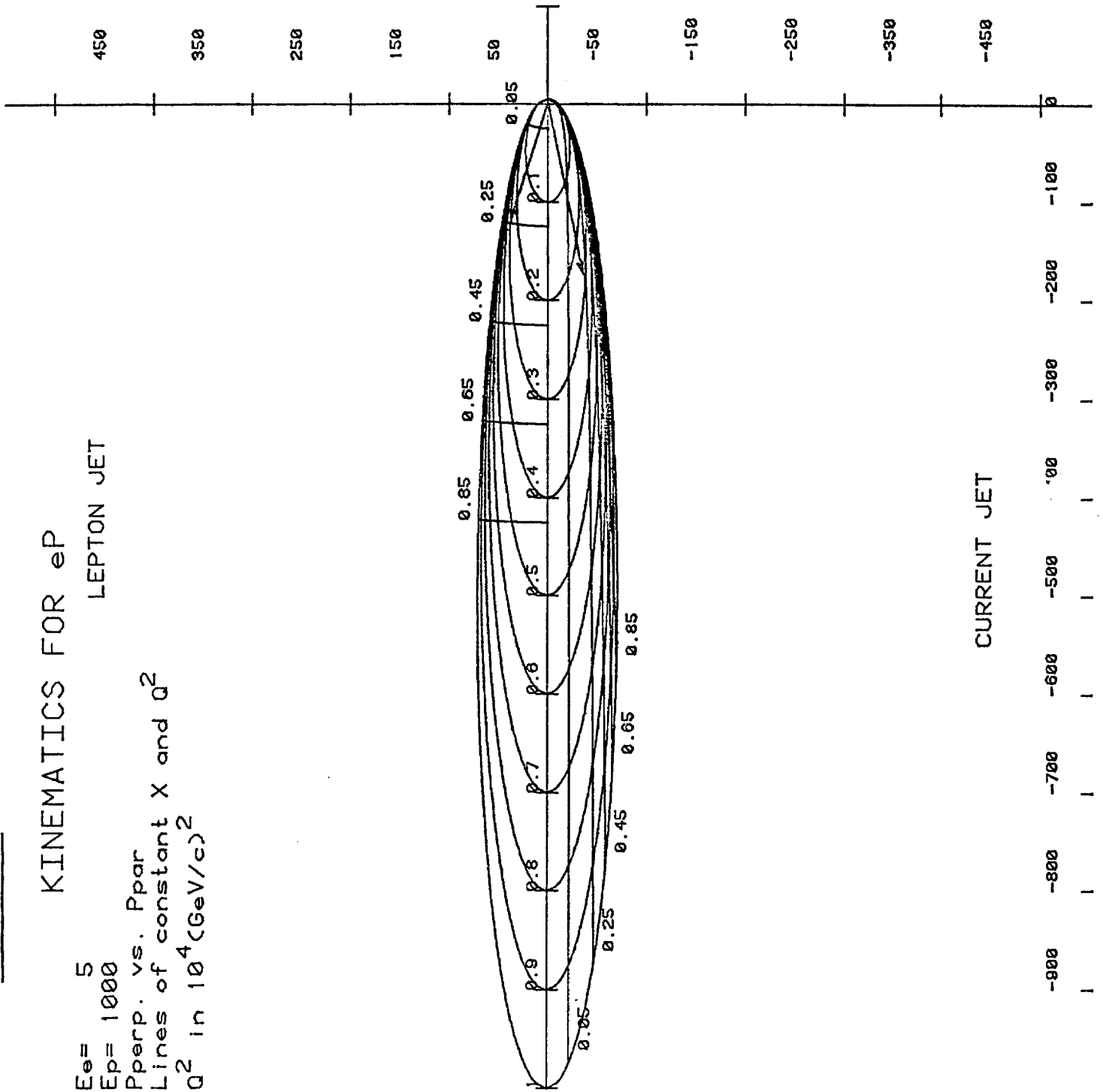


Fig. IV-1: The e-p Detector

Fig. IV-2 :

KINEMATICS FOR eP
LEPTON JET

$E_e = 5$
 $E_p = 1000$
 $P_{perp.}$ vs. P_{par}
Lines of constant X and Q^2
 Q^2 in $10^4 (GeV/c)^2$



CURRENT JET

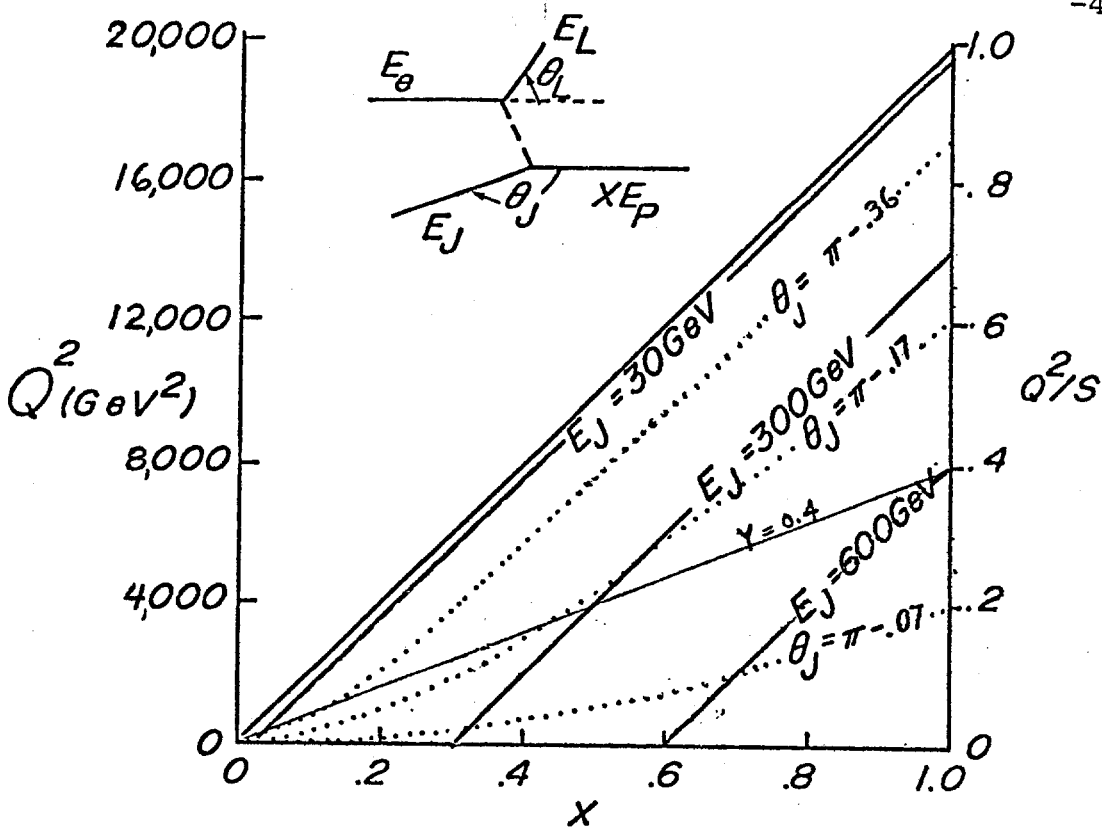


Fig. IV-3: e-p kinematics .

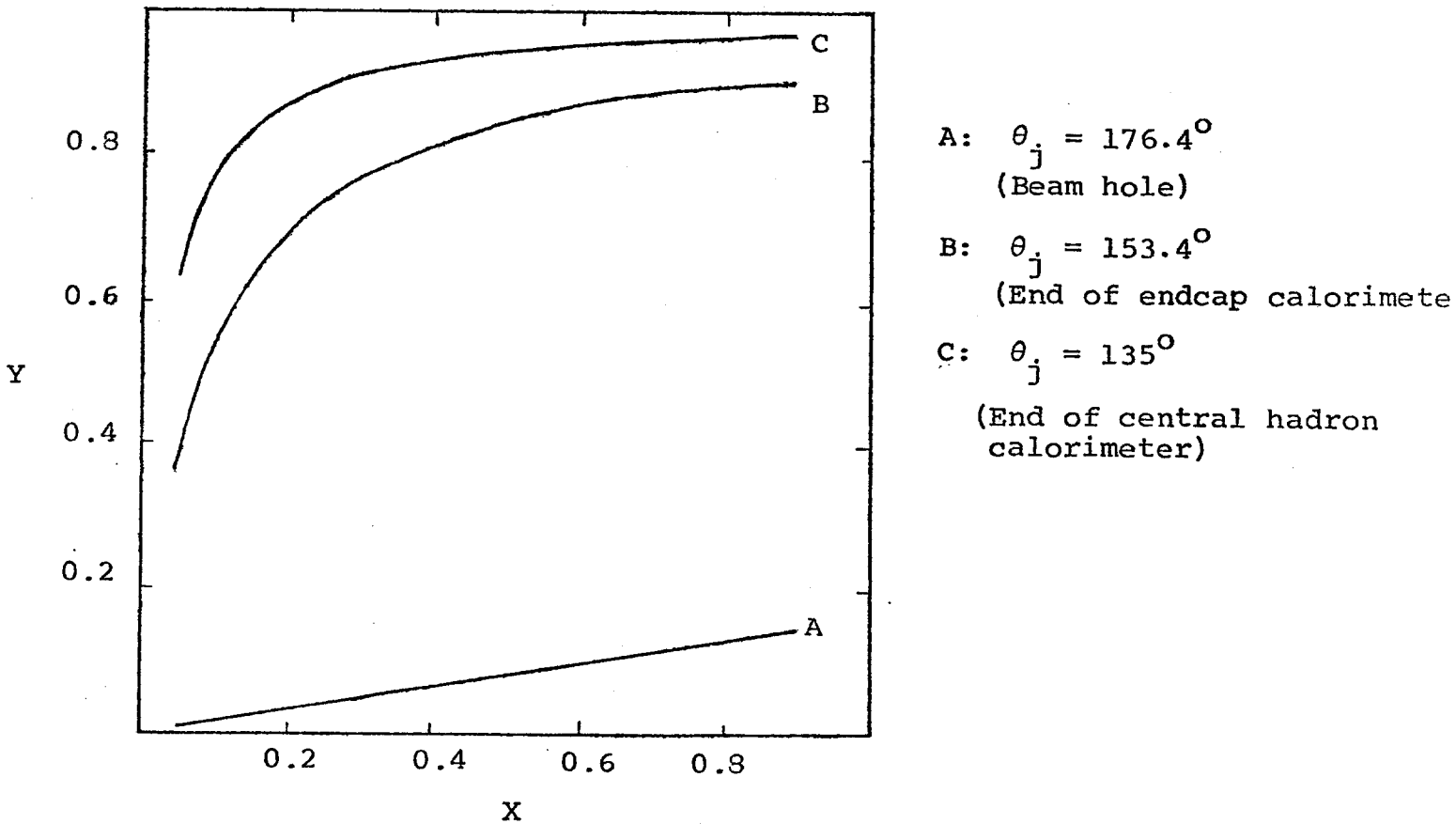


Fig. IV-5: Hadron calorimeter acceptance .

constant y , current jet angle and current jet energy are drawn on a plot of Q^2 vs. x . To reach higher Q^2 at fixed x requires increasing y ($Q^2 = s x y$). As y increases the final lepton swings more into the initial proton direction with increasing energy, while the current jet rotates away from the beam with decreasing energy. Only at very low x and high y is the current jet more than 90° from the proton direction (e.g. $x = 0.005$, $y > 0.5$).

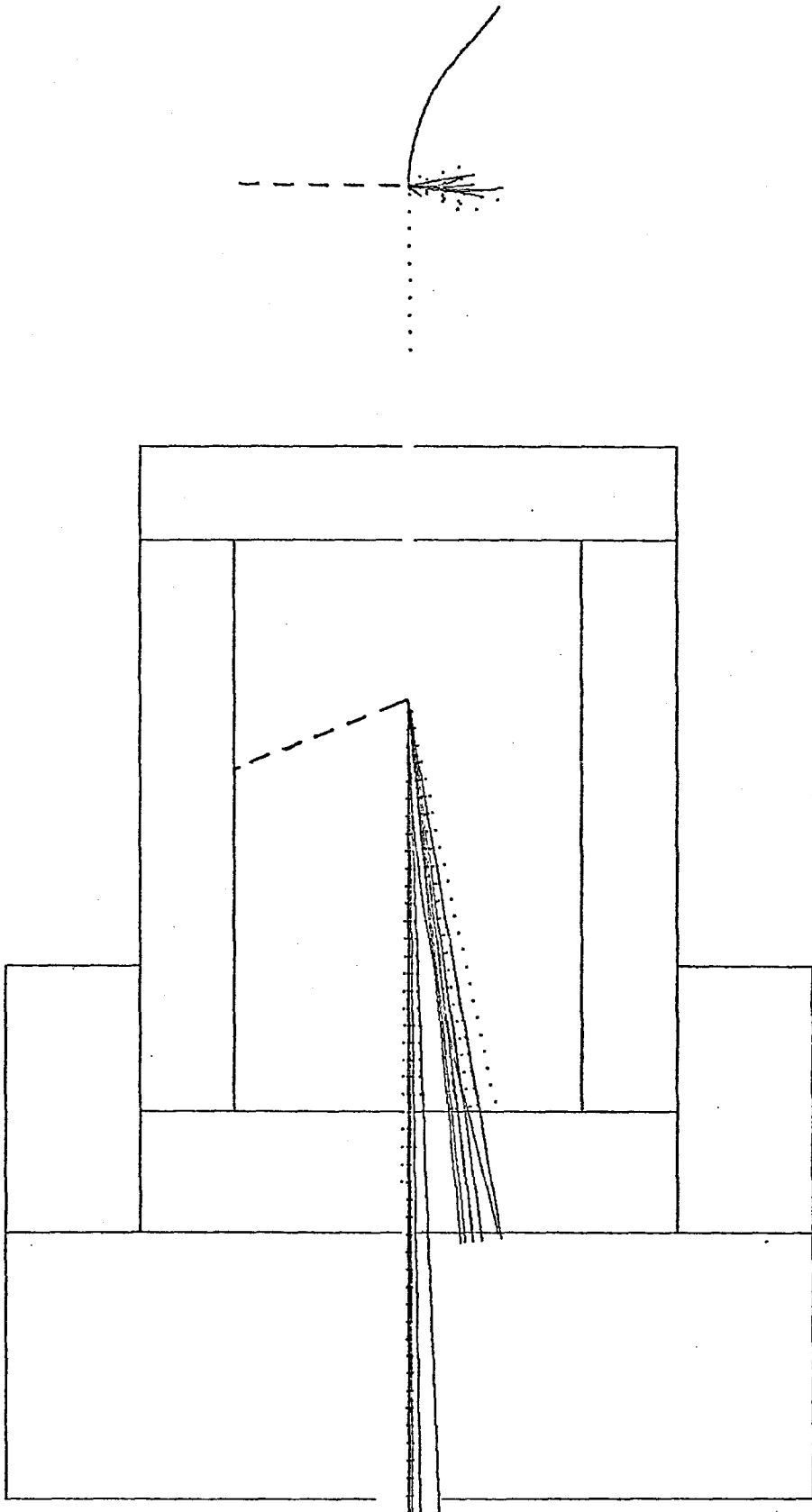
The detector must cope with a wide range of lepton and current jet energies. Lepton energies range from 5 GeV in the low Q^2 forward electron direction up to several hundred GeV at high x , Q^2 in the forward proton direction. The current jet energy range is similar, but its measurement is further complicated by fragmentation into many particles. Some typical neutral current events are shown in Fig. IV-4. Electromagnetic particles are shown as dotted lines and charged hadrons as solid lines. The events have been rotated so that the scattered lepton (dashed line) is in the upper vertical plane.

The above general considerations lead to the detector design in Fig. IV-1. The inner detector is a magnetic spectrometer with a 0.5 T superconducting solenoid field, cylindrical drift chambers in the central region and planar drift chambers in the proton direction.

Magnetic tracking is important for several reasons. It measures the momentum of the many lower energy particles

E-P EVENT

X= 0.1000 Y= 0.1000

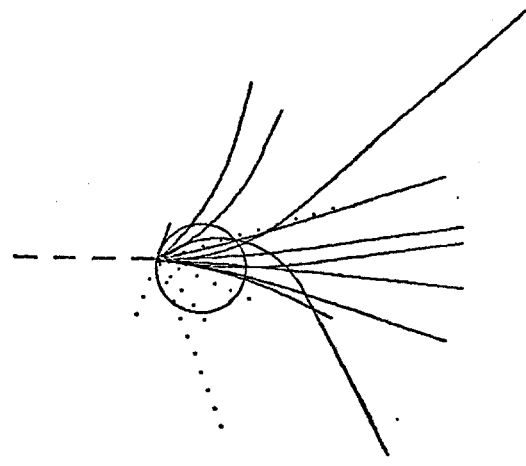
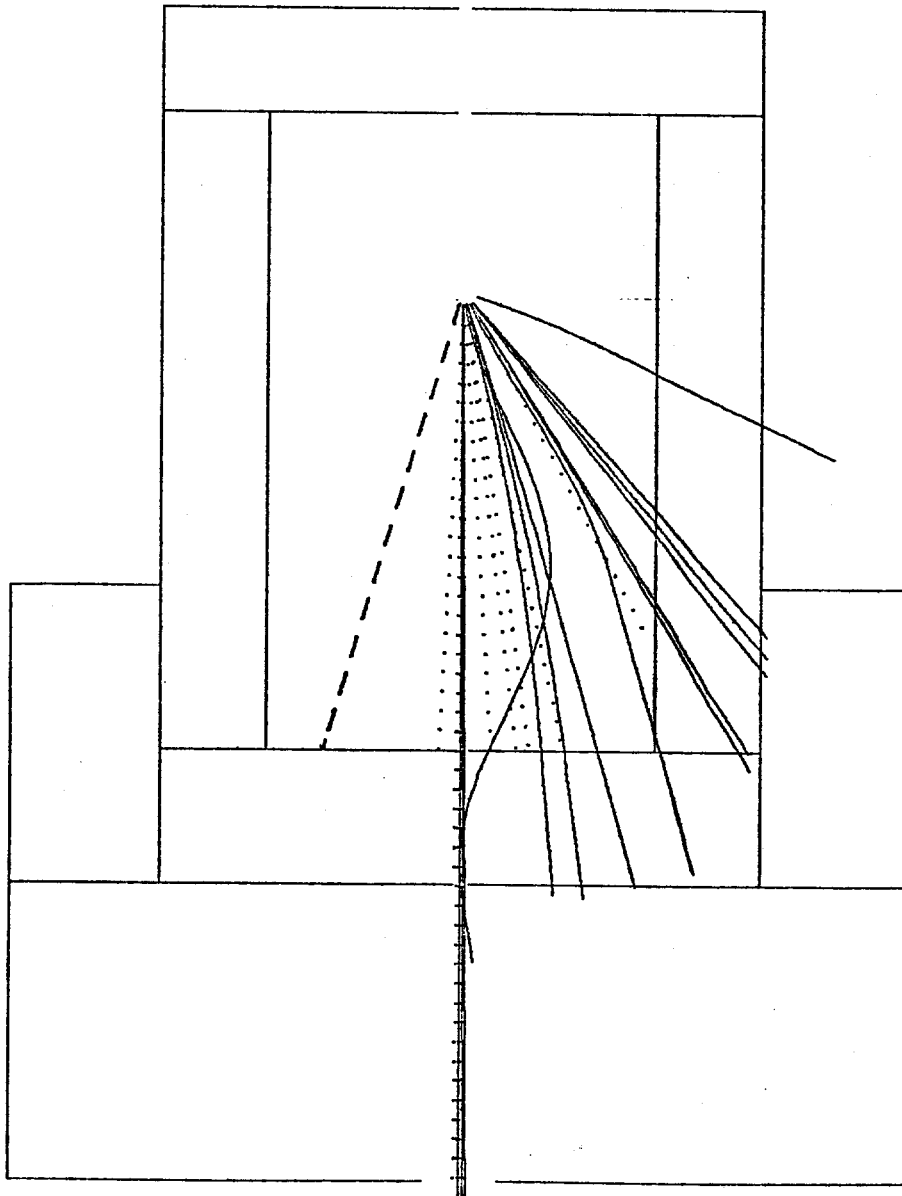


ELECTRØN ENERGY= 5.0 PRØTØN ENERGY= 1000.0

Fig. IV-4 a

E-P EVENT

X= 0.1000 Y= 0.7000

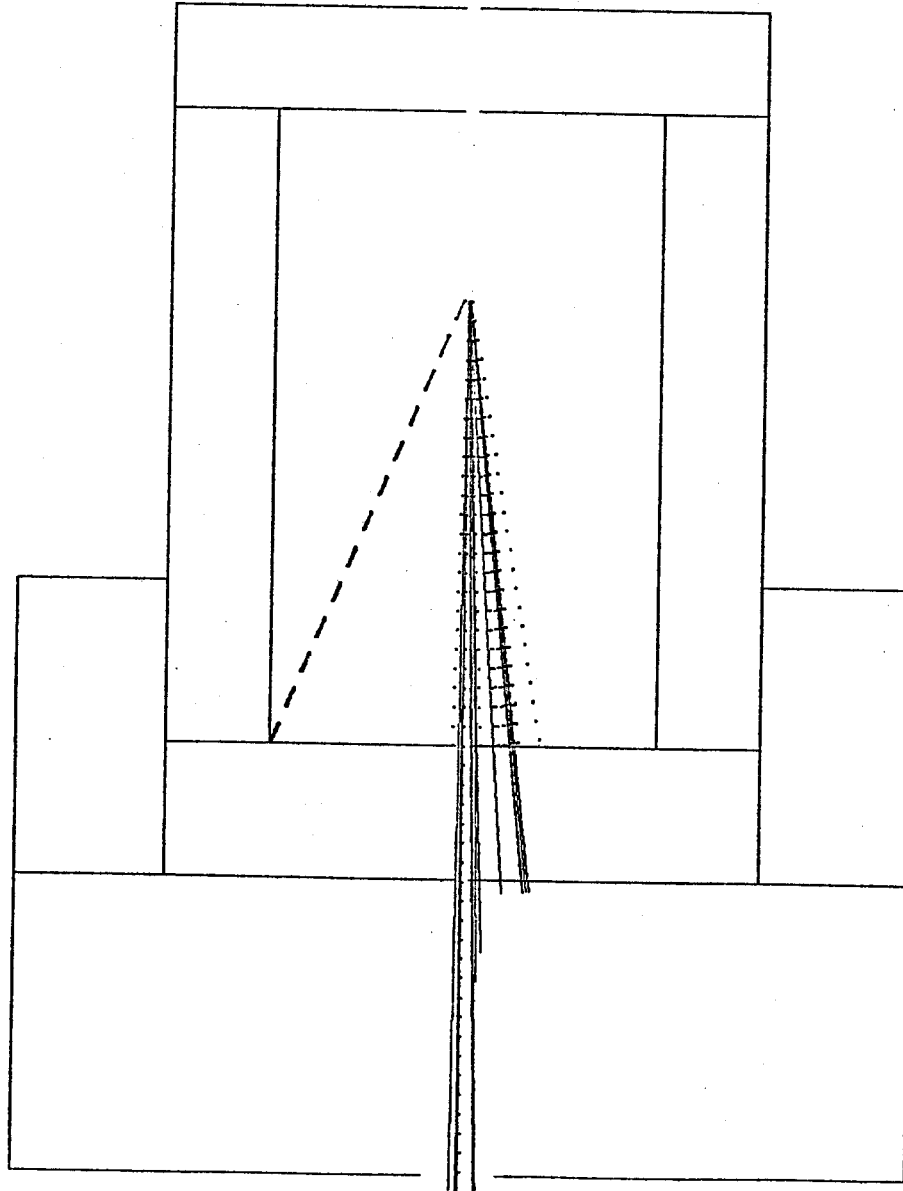


ELECTRON ENERGY= 5.0 PROTON ENERGY= 1000.0

Fig. IV-4 b

E-P EVENT

X= 0.5000 Y= 0.2000.

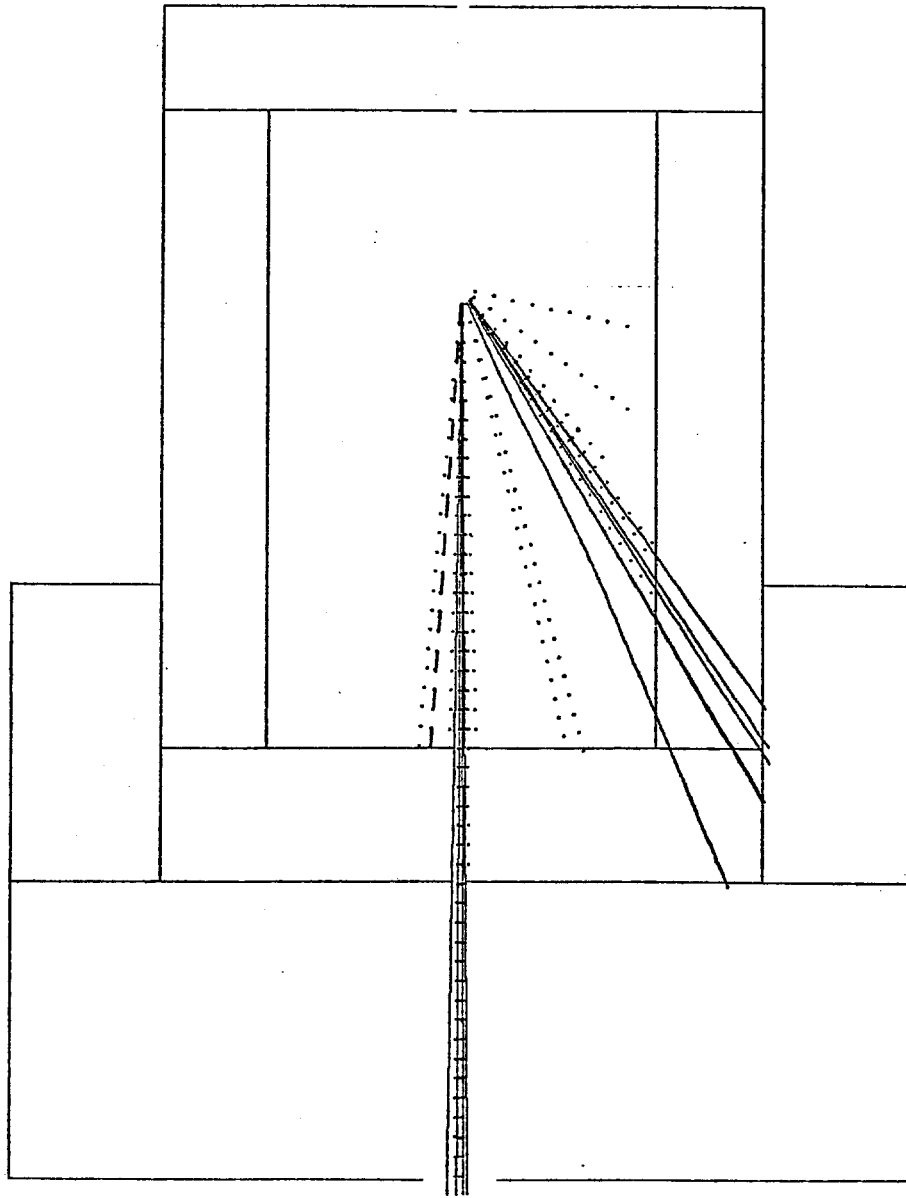


ELECTRØN ENERGY= 5.0 PRØTØN ENERGY= 1000.0

Fig. IV-4 c

E-P EVENT

X= 0.5000 Y= 0.9000



ELECTRØN ENERGY= 5.0 PRØTØN ENERGY= 1000.0

Fig. IV-4 e

in the current jet much better than calorimetry as well as generally assisting in the reconstruction of complicated events. Tracking the final state lepton is vital for separating the high rate neutral current events from charged current events. The study of heavy quark and lepton production will crucially depend on measuring the sign and momentum of muons. Finally, defining a vertex with the tracking chambers will be necessary in the trigger to suppress the background from upstream proton beam gas and beam wall interactions.

Surrounding the magnetic spectrometer with almost 4π acceptance is an electromagnetic calorimeter of good energy and spatial resolution. This will measure the scattered electron in neutral current events and also measure the π^0 content of the current jet. Measurement of the scattered electron is extended into the low Q^2 region by a system of planar chambers and an electromagnetic calorimeter. This system is also used as a luminosity monitor.

Outside the electromagnetic calorimeter is a hadron calorimeter covering the region up to 45° from the proton direction. It measures the high energy charged component of the current jet, especially close to the proton direction where the spectrometer is inadequate; it also measures the K_L^0 and neutron component. The geometry is towered for best spatial resolution. The acceptance of the hadron calorimeter is shown in Fig. IV-5 between lines and . There is a 25 cm radius hole in the calorimeter in the

proton direction to allow room for the last two quadrupoles of the electron insertion. It is expected that these can be built in a segmented way to provide some calorimetry in order to extend the low y acceptance. Beyond 45° from the proton direction the calorimetry ends, but the iron continues so that muons can be measured outside the detector in the central region.

As can be seen in Fig. IV-1, the main ring beam pipe passes through the detector. This complicates the detector design, but not unduly, and physics measurements are not compromised by its presence. The effect of the solenoid field on the main ring beam must be considered, but we believe this can be overcome by using a superconducting beam tube.

To assist in the detailed design of the detector, we have developed a Monte Carlo program which generates events using any given structure functions and fragments the final state according to the Lund model. This is a QCD string breaking model which allows the possibility of gluon jets. (The events of Fig. IV-4 were produced by this Monte Carlo program.) All particles are followed through the magnetic field to the calorimeters. An experimental error is calculated for each particle tracked by the spectrometer and for each photon and electron striking the electromagnetic calorimeter. A realistic model of showering is applied to each hadron entering the hadron calorimeter and energy

deposits in the towered grid are calculated. From this information, it is possible to try to reconstruct the kinematic variables of each event as will be done with the real data.

The problem of the neutral current contamination in the charged current events has been considered in detail. In most of the kinematic regime, the scattered lepton is well separated from the fragmenting current and target jets. Any π^0 far enough from the jet axes to be close to the scattered lepton has such low energy compared to that of the lepton that they cannot be confused. Simple cuts in the Monte Carlo program indicate that the neutral current events will always be recognized as long as the tracking and electromagnetic calorimetry is efficient, provided Q^2 of the event is greater than 100 GeV^2 .

We have applied a modified version of the Jacquet-Blondel reconstruction method to the detector using our Monte Carlo program. The Jacquet-Blondel method recognizes that it is often impossible to distinguish whether a particle belongs to the current or target jet by summing over all final state hadrons in the following equations:

$$y = \sum_i \frac{(E_H^i - P_{\parallel}^i)}{2E_e}, \quad x = \frac{[\sum_i P_{\perp}^i]^2}{s y (1-y)}$$

The contribution to y from missed target jet particles is very small and can be ignored. Even a 100 GeV particle at 20 mr contributes only 2×10^{-3} to y .

The Jacquet-Blondel method assumes that each particle can be measured individually. This will not be possible in

the calorimeter where the hadronic showers from the particles in the current jet overlap. In our Monte Carlo program, we modify the calculation of y to:

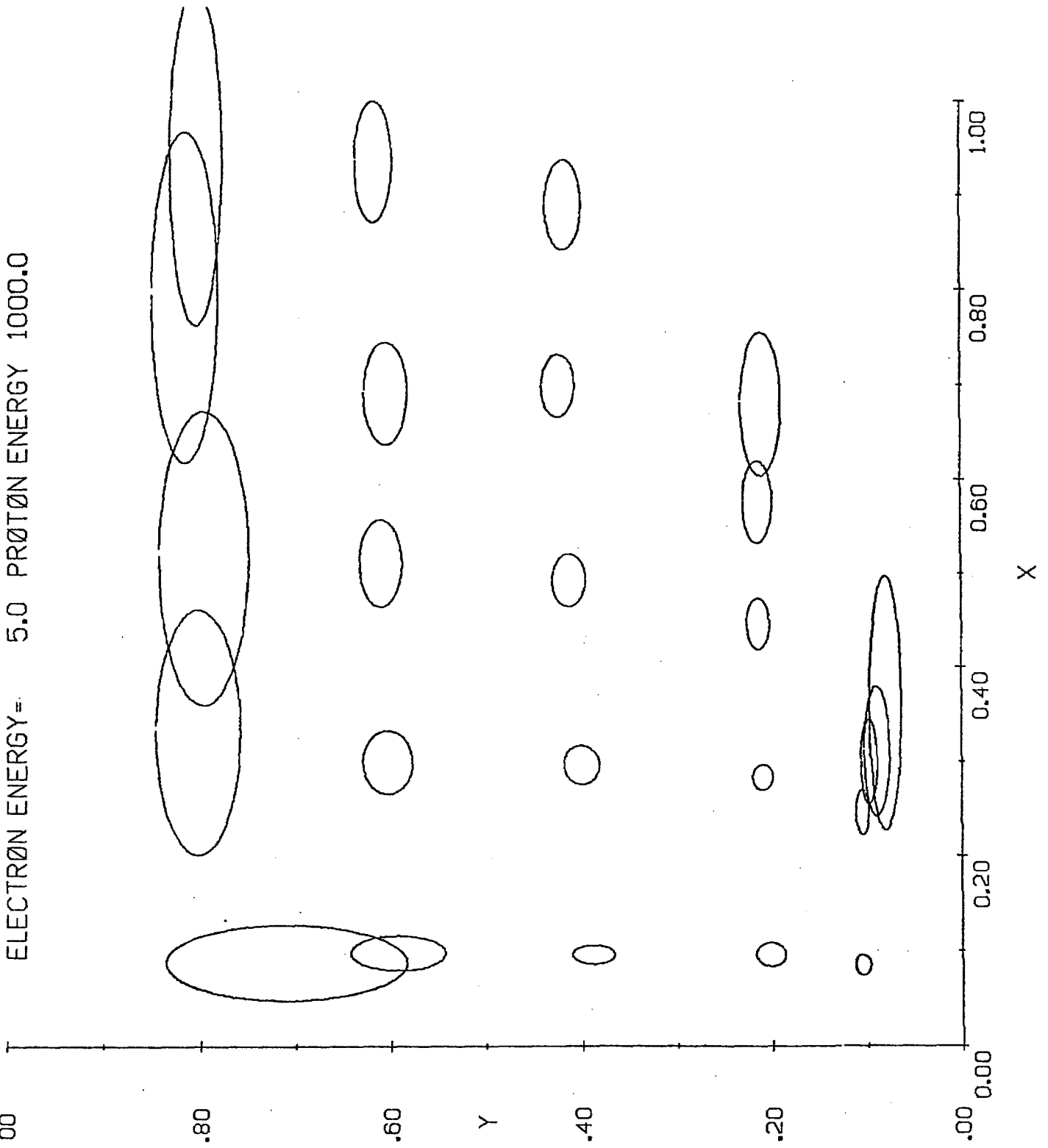
$$y = \frac{(\sum_k E_k - [(\sum_i E_k)^2 - (\sum_k P_{\perp k})^2]^{1/2})}{2E_e}$$

where k represents a grid element and E_k is the sum of the energy deposited in the k^{th} grid element by each of the final state hadrons. This equation is not exact due to the randomness of fluctuations in the jet fragmentation and in the energy measurement errors. This leads in general to an overestimate of the current jet P_{\perp}^2 using $(\sum_k P_{\perp k})^2$ and therefore an overestimate of y .

In Fig. IV-6, we plot the x, y resolution for charged current events based on this method of using the hadron calorimeter information. A 5 cm grid was used. At each of 25 x, y points ($y = 0.1, 0.2, 0.4, 0.6, 0.8$ for $x = 0.1, 0.3, 0.5, 0.7, 0.9$), 50 events were generated and reconstructed. Each ellipse is centered at the mean reconstructed x, y of the 50 events. The size of the ellipse represents one standard deviation in the distribution of reconstructed x, y . In general, measurement of x, y is good.

(The systematic overestimate of y discussed above is cancelled to some extent by loss of energy in the beam hole, which contributes to an underestimate of y .) As expected, we see gross migration and errors in the regions of low y , high x (losses in the beam hole) and high y , particularly at low x (losses beyond the central hadron

FIG. IV-6: ERRØR ELLIPSES



calorimeter). Resolution will improve, especially at higher y where typical current jet particle energies are low, when a realistic algorithm to combine the tracking and calorimeter measurements is introduced. Current effort on the Monte Carlo program is concentrated in this area.

In the final analysis, real data from the overconstrained neutral current events will show the way to the best technique for reconstructing the final hadronic state. It must be emphasized that the e - p reaction is the only collider reaction in which this constraint obtains. The neutral current data will thus provide a unique and important opportunity to study quark jet fragmentation.

V. Running Scenario

Crucial to the discussion of the physics which can be extracted from the e-p collider is the question of the anticipated integrated luminosity of the e-p experiment. In planning for the effective utilization of this facility, consideration of the competing demands from the $\bar{p}p$ and fixed target programs leads to the expectation that dedicated running in the e-p mode will be limited to about 8 weeks per year. This places a very high premium on changeover time between the various operating modes, and requires means of bringing both the electron storage ring and detector into an operating state independent of the operation of the Tevatron.

Figure V-1 shows a possible arrangement of proton quadrupoles in the interaction region which minimizes the changes involved in switching between e-p and Tev I and Tev II operation. Eight quadrupoles are added to the normal D0 straight section, giving a free space of ± 12.5 m and a β^* of 5.0 m with absolutely no changes to the remainder of the Tevatron lattice. Changeover between fixed target and e-p operation would require rolling out the extraction elements located in D0 and exchanging them with the eight proton quadrupoles shown in Fig. V-1 and the electron ring

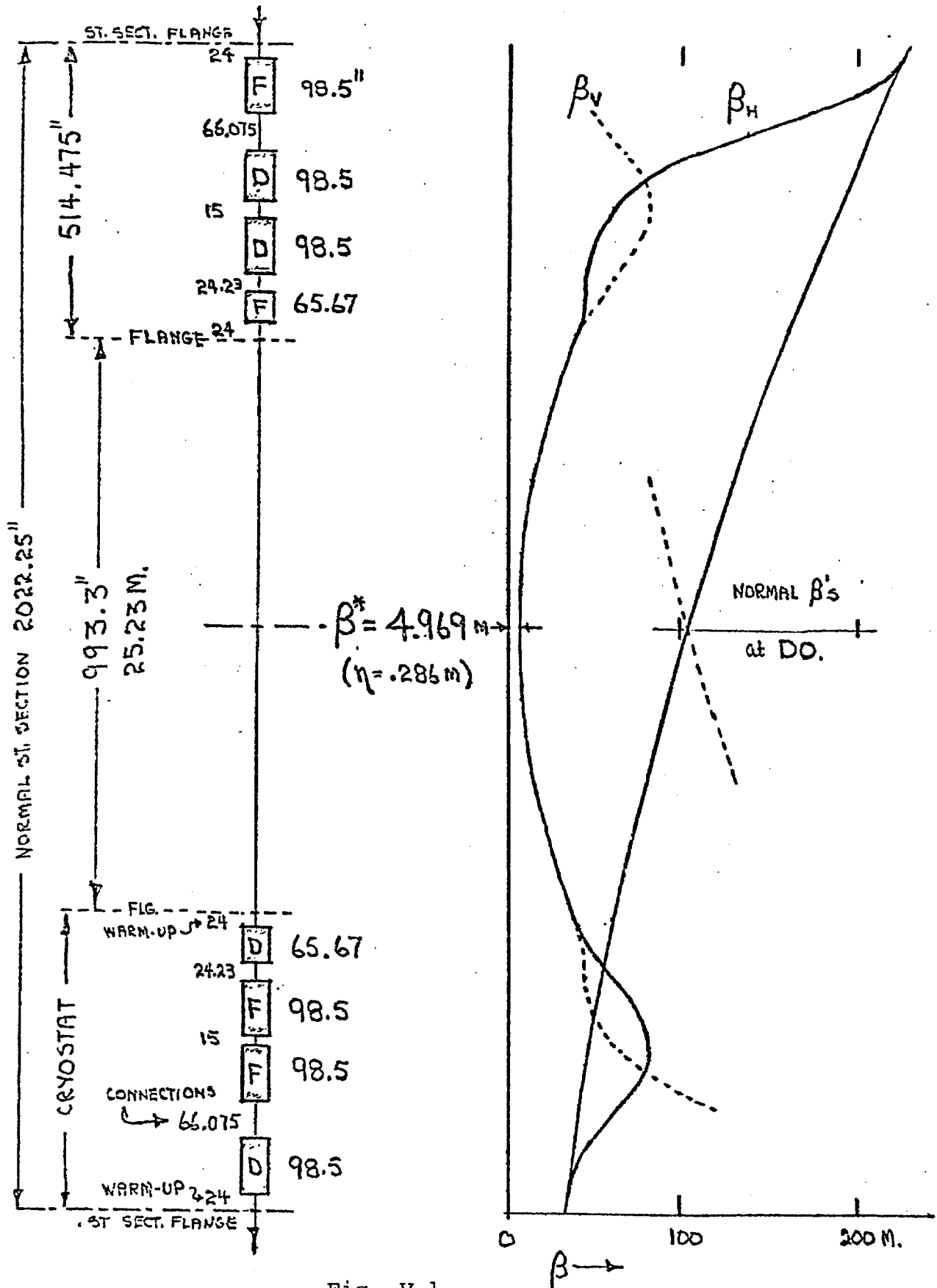


Fig. V-1

$k = .0048 / \text{inch}$ $\text{Grid} = 30.257 \text{ } \mu\text{G}/\text{inch}$ at 1000 Gey/c.

DO INSERTION.

YPC 4-82

elements shown in Fig. III-2. We would expect that these magnets would travel in and out on some sort of rail system and that no changes would be made outside of ± 26 m around the interaction region. No changeover between e-p and \bar{p} -p running would be required in D0.

The eight weeks expected to be available for e-p running in any given year is certainly sufficient time to acquire a substantial amount of data on electron-proton interactions provided that both the electron storage ring and detector are operational for the entire period. This makes a mechanism for debugging of the machine and detector during the ten months of the year in which e-p will not be running absolutely essential. This necessity is the reason that so much effort on our part has gone into the design of a suitable bypass. For the ring described here, there is sufficient space in the bypass to have the central detector located in the bypass during fixed target running.

Our view is that it is necessary to have our detector located in D0 during \bar{p} -p operation and for the e-p running period to fall at the end of a \bar{p} p run. This would provide an opportunity for debugging the entire detector, including the hadron calorimeter, and for tuning the electron storage ring in place before commencing with e-p running. (Note that the electron ring and Tevatron can be run simultaneously with no disturbance to the proton beam.) We would guess that because of the asymmetry in the e-p detector, we would be

compatible with certain classes of \bar{p} -p experiments (such as very forward spectrometers) occupying D0 simultaneously.

During fixed target operation, all electron ring elements and the detector will have to be removed from the region surrounding D0. At these times, we would expect to locate the central detector in the bypass and remove the calorimeter, muon detectors, etc. to a staging area.

VI. Costs

The cost of the present 5 GeV ring is estimated to be \$17.2 M. The cost breakdown is given in Table VI-1. We have also included in the table the cost estimate for the P 708 ring calculated under the identical assumptions as the current ring. The primary changes in our method of estimation since the submission of P 708 have been to take 50% of the technical components across the board for EDIA/Installation, and the inclusion of a 10% contingency. Note that the table does not reflect the potential savings in tunnel costs arising from excavation nearer to ground level. Also included in the table is the operating power of the ring (not including the detector). This is calculated by multiplying the rf power by two (assuming 50% efficiency) and adding on the power required to run the storage ring magnets. The required power is 1.2 MW.

The cost of the detector is estimated to be \$10.7 M. The cost breakdown is given in Table VI-2 and includes a 10% contingency.

Thus, we estimate the cost of the machine and detector for the $5 \times 1000 \text{ GeV}^2$ experiment will be \$27.9 M (1981 \$).

Table VI-1: Costs (1981 \$)

	<u>New Ring</u>	<u>P 708</u>
I. Tunnel (6.5 K/m)	\$ 3.1 M	\$ 2.3 M
II. Magnets (Incl. P.S.)		
Dipoles (103 x 13.0 K)	1.3	1.0
Quads (130 x 3.0 K)	0.4	0.5
Sext (82 x 1.0 K)	0.1	0.1
III. Vacuum (2.5 K/m)	1.2	0.9
IV. rf (0.069 V + 0.97 P)	0.8	1.1
V. Controls (800 K + 0.74 K/m)	1.2	1.1
VI. Linac (100 MeV)	1.3	1.3
VII. Booster	1.0	1.0
	<hr/>	<hr/>
	10.4	9.3
VIII. EDIA/Installation (50%)	5.2	4.6
	<hr/>	<hr/>
	15.6	13.9
IX. Contingency (10%)	1.6	1.4
	<hr/>	<hr/>
	\$17.2 M	\$15.3 M
Operating Power		
(2 x P _{rf} + P _M)	1.2 MW	1.8 MW

Table VI-2: Detector Costs

Superconducting coil and refrigeration	\$ 1.4 M
Cylindrical Chamber 8000 wires	1.6 M
Flat Chambers 8000 wires	1.2 M
Iron 930 tons	.5 M
EM Calorimeter 6000 channels	1.2 M
Hadron Calorimeter 10,000 channels	2.0 M
Tagging/Luminosity Detector	.7 M
Support Structures, General Utility, etc.	.6 M
Design, Prototyping, Testing	.5 M
10% Contingency	1.0 M
	<hr/>
Total:	\$10.7 M

VII. Summary

The construction and installation of a $5 \times 1000 \text{ GeV}^2$ electron-proton collider with associated detector is possible by the end of 1985. The physics opportunities presented by such a collider are in many areas inaccessible to either the fixed target or collider programs presently approved for the 1980's. When measured against this potential, the cost of this experiment described here is rather modest. Future extension of e-p to even higher center-of-mass energies could occur as a natural outgrowth of the presently proposed machine. We believe that it is vital that the $5 \times 1000 \text{ GeV}^2$ electron-proton collider be approved at this time.

Acknowledgments

We wish to thank several people who offered many useful criticisms and suggestions following the preparation of P 708. These include: T. Collins, R. Huson, B. McDaniel, C. Pellegrini, A. Ruggiero, R. Talman, M. Tigner, A. Van Steenbergen, and H. Wiedemann.